



Smart soil image classification system using lightweight convolutional neural network

D.N. Kiran Pandiri, R. Murugan^{*}, Tripti Goel

Department of Electronics and Communication Engineering, National Institute of Technology Silchar, Assam 788010, India



ARTICLE INFO

Keywords:
Soil type(s)
Light-SoilNet
Soil classification
Deep learning
Artificial intelligence
Hydrometer test

ABSTRACT

In the agriculture sector, soil classification plays a significant task, as it helps in soil tillage, crop selection, moisture level estimation, and automation. Conventionally, soil classification is carried out with the help of physical, chemical, and biological characteristics of the geo-referenced and mapped soil. Soil classification by conventional and laboratory methods is time-consuming, high-cost, and requires proficiency. This study presents a quick and cost-effective prediction of soil type by using soil images. A soil image dataset has been created to classify the soil type using images. To create the soil image dataset, 392 soil samples are collected from different agricultural fields in Andhra Pradesh, India. The collected samples are dried and the soil type is identified using a sieve and hydrometer analysis in the laboratory. An imaging setup has been made to capture the images of the dried soil samples using a smartphone camera. The captured images are pre-processed using: RGB extraction, and V extraction from HSV bins, and adaptive histogram are applied to highlight the texture features of the soil images. A novel lightweight convolutional neural network called Light-SoilNet is proposed to classify five soil sample images: sand, clay, loam, loamy sand, and sandy loam. The proposed network is designed to take care of the imbalanced soil image dataset. The proposed network is tested and compared with state-of-the-art lightweight and pre-trained deep learning networks. The proposed Light-SoilNet network architecture has produced an overall accuracy of 97.2% in classifying the soils. The comparison of the results shows the performance of the proposed model using the image and deep learning techniques in classifying the soil types.

1. Introduction

Due to population growth, the amount of land available for agriculture has decreased in recent decades. With the rising population, there is a need to increase food grain production with viable land. Many agricultural innovations, such as the “Green Revolution,” have been implemented in recent decades to enhance crop yield by modifying the genetics of the plant or crop to meet the food demand (Liu et al., 2020). The new green revolution can no longer be realized, posing health risks (Cervantes-Godoy et al., 2014), like reducing infant mortality by 2.4 – 5.3 using modern crop varieties (von der Goltz et al., 2020). Researchers are looking at the soil as an alternative for boosting agricultural output. Crop selection depending on soil type must be made to increase production (Dorothee Spuhler and Nina Carle, 2019; Soil Types: A Main Aspect Of Agricultural Productivity, 2019). Initially, soil classification has to be made a practice for crop selection (Haider et al., 2019).

In geotechnical engineering, classifying the soil type based on conventional methods is time-consuming, high cost, and requires

proficiency for analysis. In recent years, the research of soil type classification in agriculture for crop selection has been a relevant topic. Researchers have stated techniques for soil classification based on environmental factors such as temperature, wetness, humidity, pH, soil fertility, mode of formation, and soil structure/texture (David et al., 2018). Developing a reliable system that is applicable to a large number of classes is a very challenging task. Several studies have been using a few classes for the classification of soil type. Soil texture plays an important role in classifying the soil type. The soil texture varies with the percentage change in sand, silt, and clay in the soil sample. The water-holding capacity of the soil depends on the texture of the soil. The amount of leaching of the nutrients from the soil depends on the water-holding capacity of the soil, which has an impact on crop production. Texture generally refers to how rough or smooth the soil is. Farmers try to know the texture of the soil profile by feeling the roughness and smoothness of the soil. To know the texture of the soil, geotechnical engineers use conventional methods like sieve analysis, hydrometer test, pipette analysis and many other laboratory methods (Fomin et al., 2021;

* Corresponding author.

E-mail addresses: d_rs@ece.nits.ac.in (D.N. Kiran Pandiri), murugan.rmn@ece.nits.ac.in (R. Murugan), triptigoel@ece.nits.ac.in (T. Goel).

[Lu et al., 2000; Alary et al., 2013](#)). Based on the texture, sixteen soil types are present, in which few of them look similar, which makes it difficult to identify the soil type. However, analyzing the soil samples and acquiring information is still a bottleneck, which includes many hours of experimental manual work by proficiency and require high-cost equipment involved in identifying the soil type. There is a need of cost-effective methods to identify the soil type by reducing the economic burden to farmers. Computer vision along with the artificial intelligence has unlocked the barriers in identifying minute patterns and automation of the systems. In this paper, we have adopted image analysis in identifying the soil type, which is cost-effective and reduces the man-power and time. The automatic classification of soil is still a challenging task for researchers.

In recent times, convolutional neural networks (CNN) are playing a major role in detecting the texture features from the image ([Gómez-Ríos et al., 2019](#)), and deep learning (DL) models have been successful in identifying the texture features or pattern of an object in an image. The depth of the deep learning depends on the application or problem specific ([Zhang et al., 2018](#)). As the depth of the networks increases, the DL models can extract complex features much more effectively. With the knowledge of geotechnical engineers to increase the efficiency in classifying the soil type with high precision or accuracy, we have proposed texture-based imaging and a DL model. DL algorithms are generally data-hungry and require more images to train the model. In this paper, we have proposed a novel lightweight CNN model named Light-SoilNet network, which can process an imbalanced small soil image database ([Zhang et al., 2023](#)) by reducing the number of learnable parameters, and FLOPs and avoiding overfitting in classifying the soil images with better performance. The proposed model reduces the computational complexity and increases the performance by reducing the learnable parameters of the proposed network. Part of the soil images database created for classification is made publicly available ([Kiran et al., 2021](#)).

The following are the key contributions of this work:

- Development of soil image database by capturing the images with a smartphone and labelling based on the laboratory analysis by following specific standards.
- Rather than classifying the gravel and aggregate soils, classified the soil types like sand, clay, loam, sandy loam and loamy sand related to agriculture soils.
- HSV, RGB extraction, and adaptive histogram techniques are applied to the database to highlight the texture features of the soil sample images.
- Developing a novel Lightweight network aimed to classify the soil images with less number of layers, learnable parameters, epochs, size of the network, and better performance.
- The performance metrics of the proposed model are evaluated by comparing them with the pre-trained, lightweight networks and state-of-the-art-model.

In the proposed model, dropout layers are included to overcome overfitting during the training process.

The remaining part of the paper is organized as follows: [Section 2](#) describes the related work, [section 3](#) includes materials, [section 4](#) presents the methodology proposed, [section 5](#) presents experiment results, and [section 6](#) provides the discussion and performance analysis. The conclusion and future work are presented in [section 7](#).

2. Related work

Classification of soil based on its texture, and physical and chemical properties is a challenging task in any field related to soil science. As these properties vary to environmental conditions, researchers have to follow specific standards in creating the dataset and designing the model. This section is divided into three where the first two sub-section discusses about the models where the authors used their own soil images

database and existing database in the public domain in classifying the soil type while the last sub-section discusses about the Light-weight CNNs in classifying the soil types.

2.1. Soil image database

In ([Azizi et al., 2020](#)) transfer learning approach was considered in classifying the soil aggregates using stereo-pair images. The pre-trained networks VggNet16, ResNet50, and inception were taken and the classification was done based on the mean weight diameter (MWD) of the aggregate soils. In this model, soil classification was done based on the parameter of MWD, which cannot be used in classifying the soil types clay, silt, loam and other soils with small particle sizes. ([Inazumi et al., 2020a](#)), a simple deep CNN model used to identify sand, clay, and gravel. The images of the soil sample are taken using a high-resolution mobile camera. The authors concentrated on standard soils rather than agricultural soils and the dataset is imbalanced data. In ([Yu et al., 2019](#)), used spectral images in the classification of five types of soils based on color by using 3D-CNN and principal component analysis (PCA). The spectral images were captured by using a CMOS camera with liquid crystal tuneable filters and digital mirror devices. The PCA was applied to reduce the dimension of the spectral images.

In ([Reale et al., 2018](#)) proposed a system for automating fine-grained soil detection in construction in-situ. A two-layered feed-forward neural network was used to automate soil classification using European Soil Classification System (ESCS) and Unified Soil Classification System USCS. The network was trained using the Levenberg-Marquardt back-propagation algorithm to detect fine-grained soils. Granular soil prediction is ineffective since consistent prediction is not possible. The plasticity index has the most inaccurate ANN predictions. ([Mengistu & Alemayehu, 2018](#)) proposed a back-propagated artificial neural network to characterize the soil type by measuring the soil moisture level. The images of the soil were captured by using a digital camera, and the moisture levels of the soil were measured by using the Gravity Analog Soil Moisture sensor. Classification of soil based on the moisture sensors can be affected by the conductivity and other soil chemical properties. This leads to the error in measuring the moisture levels and soil classification based on this feature, which gives inappropriate results. ([Uddin & Hassan, 2022](#)) created a soil image dataset by collecting samples from the Mymensingh division, Bangladesh. Eight soil types were collected, and for each soil type, only one sample was collected to classify the soil type. Each soil type's images were augmented, and HOG, Haralick, RGB, HSV, and L*a*b features were extracted. The features were classified by using ML classification algorithms. The SVM classifier achieved better performance. From each soil image, 4864 images were generated by augmentation, which leads to overfitting, and the model performance will be high in training. The model's performance was high because the same images were used for testing. The researchers have used deep neural network models to classify soils like aggregate soils of size varying from 7 mm to 110 mm diameter, granular, sand and clay soils. These models may give inefficient results in classifying other types of soils. In ([Azizi et al., 2020; Mengistu & Alemayehu, 2018; Reale et al., 2018](#)), researchers used physical and chemical parameters to classify the soil type, which cannot be applied to soil particles of size less than 75 μm .

2.2. Online database

In ([Jagetia et al., 2022](#)), the authors proposed a Visual Transformer (ViT) with eight transformers and two heads that performed well. The dataset used for classification was collected online, which contains 1000 images of four soil classes. The images of the dataset were captured without following any standards. For ViT, a minimum of 10 million images were required to train the model. The low collected dataset was augmented to create a huge database, which would lead to overfitting. In ([Chatterjee et al., 2021](#)), a comparative analysis in classifying the soil



Fig. 1. Represents the areas where soil samples are collected. (a) Rajahmundry (b) Madanapalle.

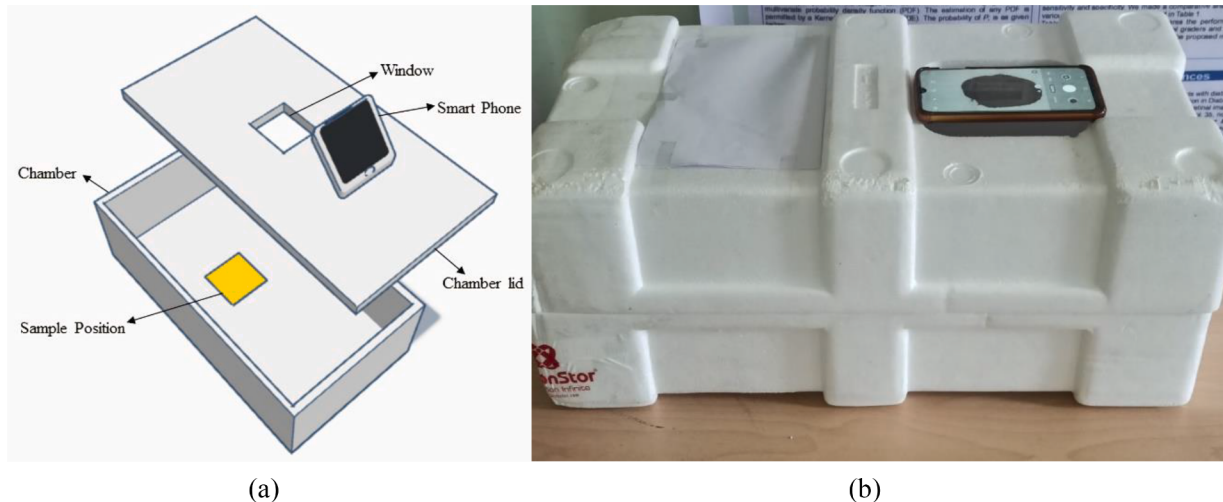


Fig. 2. Image acquisition setup. a) Isometric view of a chamber and b) Styrofoam box to capture images.

types using different pre-trained networks was conducted. Four soil types: Red, Black, Alluvial, and clay, were identified based on the colour and texture by using an online soil image dataset. The soils were classified using ResNet50, VGG19, MobileNetV2, VGG16, InceptionV3, and NASNetMobile. The networks identified the alluvial soil as black and clay soils due to the colour and texture of the alluvial soil. (Lanjewar & Gurav, 2022) developed a simple CNN architecture and evaluated the model by comparing it with various deep CNN architectures. The existing online database was used to classify the soil types. In (Chatterjee, 2021; Jagetia, 2022; Lanjewar & Gurav, 2022), the authors used an online database created by collecting images randomly from various sources. The database does not follow standards in capturing the images.

2.3. Lightweight CNN

A lot of recent work has been done and tried to figure out to minimize the CNNs while simultaneously enhancing their performance and inference speed (He et al., 2015; Denil et al., 2013; Han et al., 2015; Wu et al., 2016; Cheng et al., 2017; Gong et al., 2014; Howard et al., 2017). Many of these methods involve pruning or compressing the size of CNNs and reducing the computational time. For real-time face recognition, (Chen et al., 2023) a lightweight CNN was designed by using an inverted residual shuffleNet model, to diagnose the COVID-19 chest X-rays (Yang et al., 2022) a lightweight CNN based on DenseNet was implemented, and (Zhao et al., 2022) by leveraging the MobileNetV2, a lightweight

network was designed to improve the performance of the model. In all these methods, researchers intended to reduce the pre-trained models rather than implement smaller and faster deep learning networks. The pre-trained networks inherit the limitations, where the input image sizes are pre-defined, and the networks are unable to handle random-sized images as the dimensions of the convolutional feature extraction block rely on the input image size.

In the proposed model, we have addressed the issues by creating a soil image database and labelled the soil type based on the texture of the soil. We have used texture in identifying the soil type rather than physical and chemical properties. The created database images are labelled based on the texture of the soil, which is identified by conducting laboratory experiments. We have designed a deep lightweight network for soil classification rather than compressing the existing pre-trained networks.

3. Dataset creation

This section discusses acquiring the soil samples, creating a soil image database, and analyzing the soil samples in the laboratory.

3.1. Acquiring soil samples

For the classification of soils, ninety-six soil samples are gathered from agricultural fields in various locations, covering two different

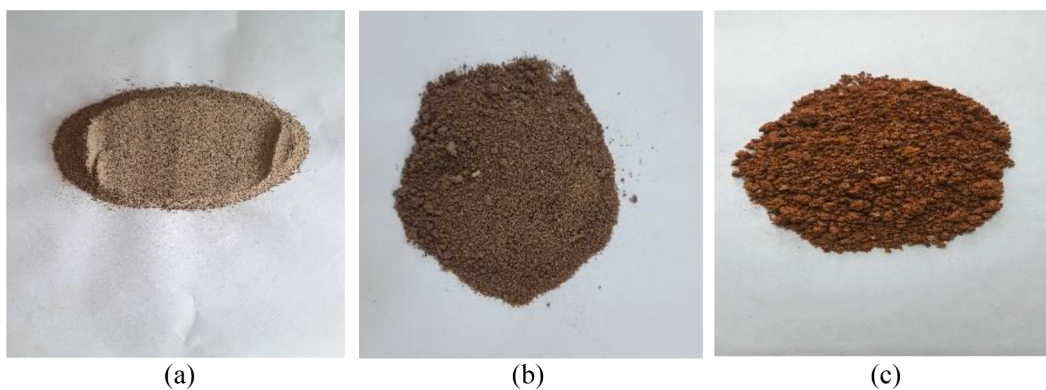


Fig. 3. Represents the clay, loamy sand, and sandy loam soil images captured using a smartphone camera.

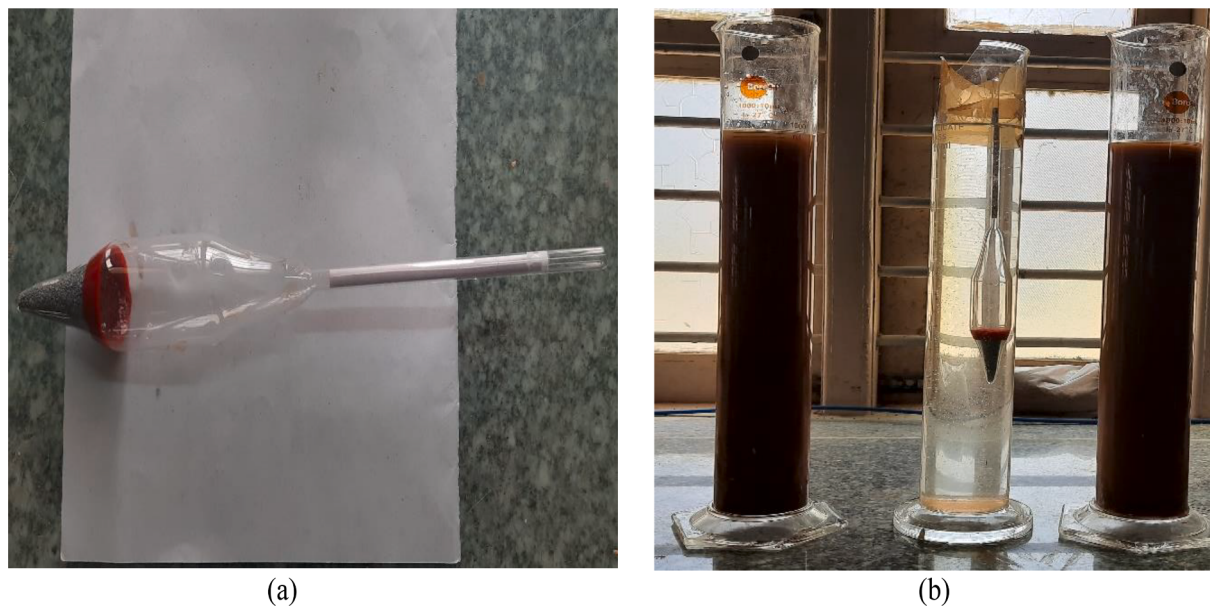


Fig. 4. A) hydrometer. b) hydrometer testing equipment for testing the soil texture.

ecological regions of Andhra Pradesh. The regions include the Godavari River coastal zone, rich in alluvial and sandy soils and drought-prone areas with sandy and rocky soils. The coastal region is good for paddy, and the other region is suitable for vegetable cultivation. The soil samples were obtained at a depth of 5 to 10 cm below the field surface. The locations of the acquired samples are 16°59'24.5"N latitude and 81°48'54.9"E longitude and 13°56'07.4"N latitude and 78°47'95.5"E longitude. The collected soil samples are further divided into 392 samples. Fig. 1 shows the areas where soil samples are collected. The hydrometer test and sieve analysis procedures are used to determine the percentage of sand, silt, and clay in each sample obtained under the supervision of the Department of Civil Engineering, Madanapalle Institute of Technology & Science (MITS), Madanapalle, India. The measured values are plotted on the USDA triangle to determine the texture of the soil samples.

3.2. Soil image dataset

To develop the soil image dataset, the images of the acquired soil samples are captured by using a Samsung smartphone camera. Before acquiring the images, the organic components present in the soil are removed, and the moisture content is removed by drying the soil in a hot air oven at 100 °C for 24 h. A chamber with dimensions 45x20x10 cm was constructed with Styrofoam to capture the images. A window of

dimensions 14 cm × 10 cm was made on the top of the box to place the soil sample inside the box and allow low light for capturing the images. As the box walls are white, allowing the light that enters the box through the window will provide the illumination conditions enough to capture the soil images without affecting the actual color of the soil. The mobile device is placed at a height of 10 cm from the soil sample base and captures the images. Fig. 2 shows the setup made to capture the soil images.

The images of the thirty-two soil samples are acquired to create the dataset for soil classification. The soil images are captured using a smartphone camera with 48 megapixels. The camera has an ISOCELL GM2 sensor with an f/2.0 aperture lens. The ISOCELL imager provides mobile device users with a broader, clearer viewing experience. The Smart Wide Dynamic Range (WDR) technology of ISOCELL can capture the details more accurately in both bright and dark areas, even in high-contrast lighting conditions. The soil images are augmented to create the Indian Regions Soil Image Database (IRSID) (D N Kiran et al., 2021), a part of the dataset created that was made public in the research work. Fig. 3 shows the sample soil images that are captured. Fig. 4.

3.3. Soil analysis in the laboratory

Each soil sample is subjected to laboratory examination to determine the texture of the collected soil samples and label the soil type by

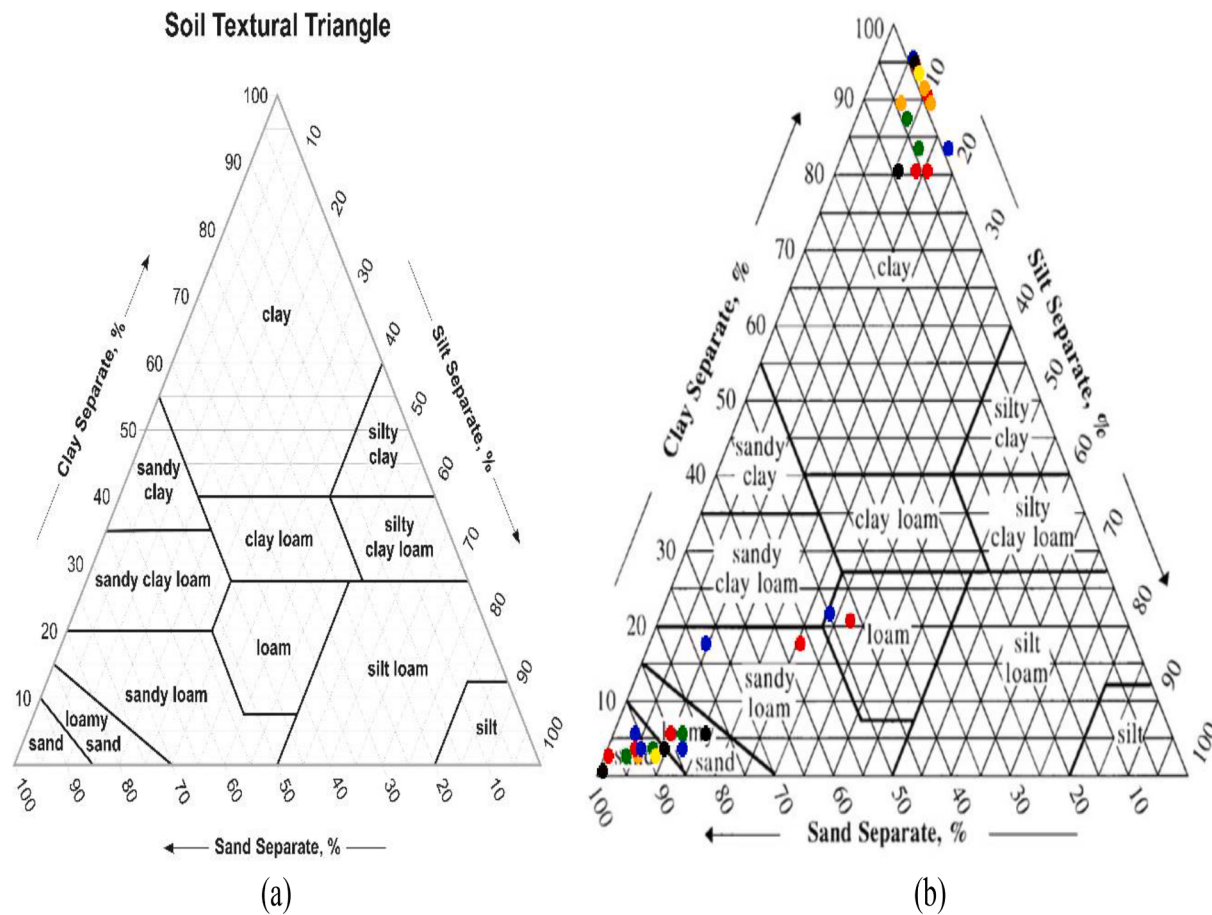


Fig. 5. A) USDA texture triangle for classification. B) USDA texture triangle with some soil samples plotted.

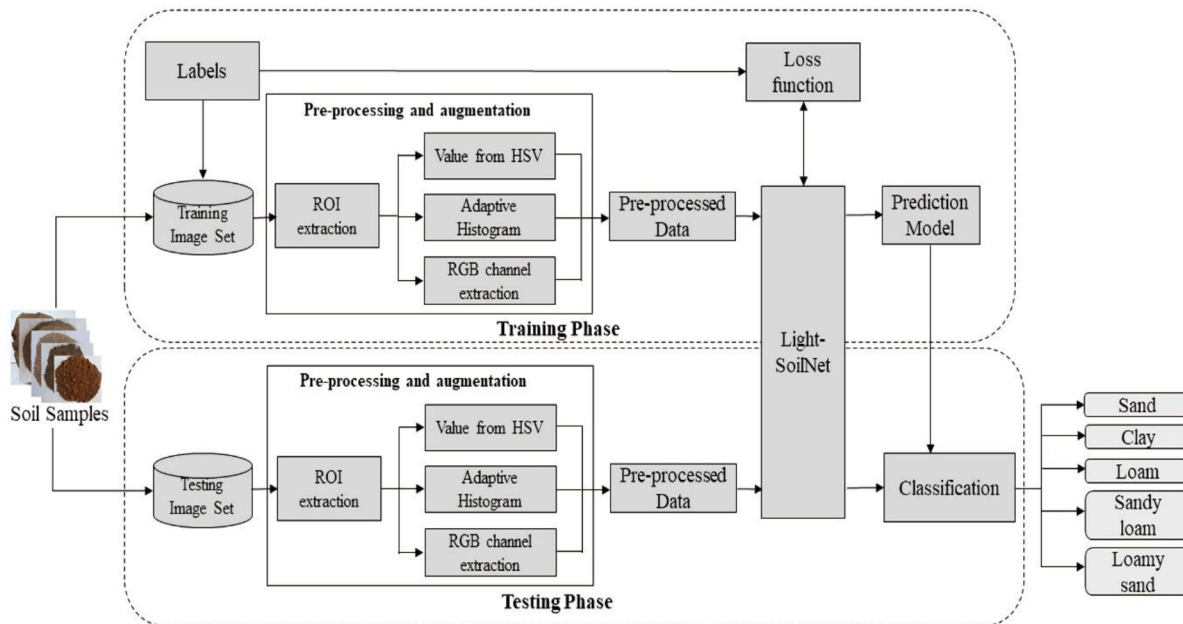


Fig. 6. The workflow of the proposed model in the classification of soil.

identifying the fraction of sand, silt, and clay. For sandy soils, sieve analysis is used to identify the fraction of sand, silt, and clay, whereas, for loamy and clay soils, a hydrometer test is used to determine the percentage of sand, silt, and clay.

The sieve analysis and hydrometer test are done in the department of civil engineering laboratories, MITS, Madanapalle, Andhra Pradesh, India. In sieve analysis, 500gms of sand-type soils are taken and sieved through the different sieve pans of sieve sizes up to 75 μm to find the

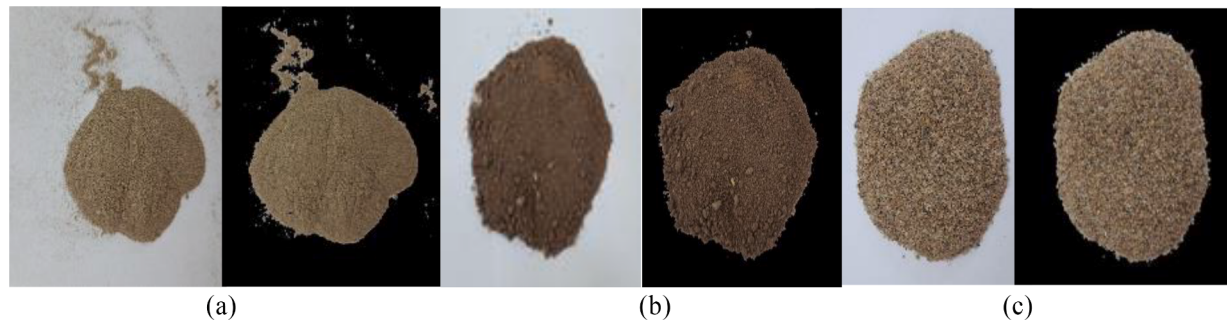


Fig. 7. a, b, and c represent the clay, loamy sand and sand images and the corresponding ROI images.

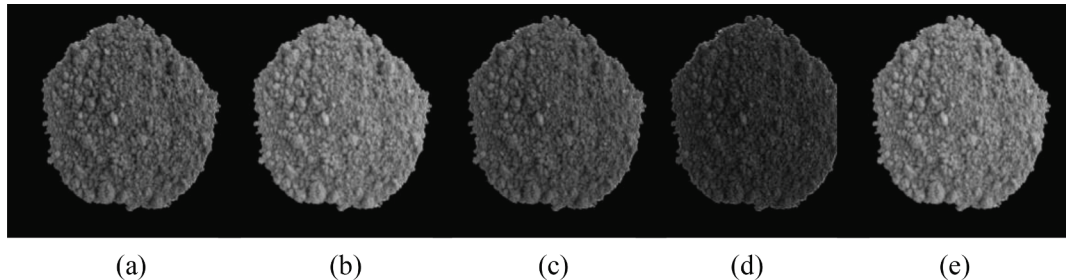


Fig. 8. Sample Pre-processed images. (a) Adaptive histogram. (b-d) RGB channels respectively. (e) V extraction from HSV.

fraction of sand. If the fraction of silt and clay that passed through the $75\text{ }\mu\text{m}$ sieve pan is greater than 10 percent, we conduct a hydrometer test to find the silt and clay fraction.

Before starting the hydrometer analysis test, the hydrometer has to be calibrated. The hydrometer is immersed in a glass cylinder of size 1 L filled with 800 ml water to measure the volume of the hydrometer and to calculate the effective height of the hydrometer (H_e). The effective height of the hydrometer is measured for each reading present on the hydrometer (R_h). Eq. (1) shows the effective height measured for hydrometer calibration. The measured effective height (H_e) and R_h values are plotted to check the hydrometer's effectiveness. By mixing 33 gms of sodium hexametaphosphate and 7 gms of sodium bicarbonate in one litre of water, a solution is made and left for 24 h. The solution acts as a dispersion agent in preventing the fine particles in the suspension from clumping together. Now, 100 ml of the solution is mixed with 800 ml of water for the hydrometer test. In the 900 ml prepared solution, 50gm of the tested soil sample is added, and readings are taken at regular intervals over the following 24 h. The entire procedure follows all the steps of the hydrometer test (Sashi Gulhati and Ranjan, 1986; Backus, 2018). The height of the hydrometer from the surface of the solution is recorded at regular intervals. Finally, the texture of the soil sample is determined by plotting the percentage of sand, silt and clay on the United States Department of Agriculture (USDA) texture triangle (USDA, 2013). Fig. 5 depicts the USDA texture triangle and the USDA texture triangle with soil samples plotted on it.

$$H_e = H + \frac{1}{2} \left[h - \frac{V_h}{A} \right] \quad (1)$$

H = length from neck of bulb, to graduation R_b , in cm;

h = twice the length from the neck of bulb to its centre of volume, in cm;

V_h = volume of hydrometer bulb, in ml;

A = area of measuring cylinder in cm^2 .

4. Methodology

In this section, we discuss the methodology to classify the soil type using Region of Interest (ROI). The general workflow of the proposed model is shown in Fig. 6. The general workflow includes the following steps: extracting the ROI of the soil images, pre-processing and augmentation, and Light-SoilNet in classifying the soil images. The soil dataset has been processed to extract the ROI of the soil images. To highlight the texture and augment the data, ROI images are pre-processed.

4.1. Image pre-processing and augmentation

The dimensions of the soil images captured are 2992x2992, and the size of the images is 2.25 MB on average. To reduce the computational complexity of the proposed model, an optimal image size 728x728 has been chosen where the loss of information is less when compared with the image of size 512x512. In this stage, the region of interest (ROI) of the images has been extracted to distinguish the soils from the background. The HSV color threshold (Jayanthi and Iyyanki, 2019) technique has been applied to extract the ROI of an image. Fig. 7 shows the acquired and ROI-extracted images of the soil. The tool used to extract ROI from images is MATLAB2021a.

The soil texture is the indication of the relevant content of particles of various sizes in the soil. Based on the texture of the soil, the soil has been classified. To highlight the texture features of the soil images and increase the soil image database for training and testing the Light-SoilNet network, various pre-processing techniques have been applied to the ROI images of the soil for detecting the texture features by the Light-SoilNet model. The pre-processing techniques are as follows: adaptive histogram, extracting the Value from the HSV image and extracting the RGB channels separately from the grayscale ROI images.

The images are converted into greyscale to perform an adaptive histogram because of the significant color shift when performing the histogram equalization independently on the images red, green, and blue components. The adaptive histogram images enhance the edges of the images, which helps identify the texture of the soil images (Sudhakar, 2017; Singh et al., 2016). The number of soil images generated after

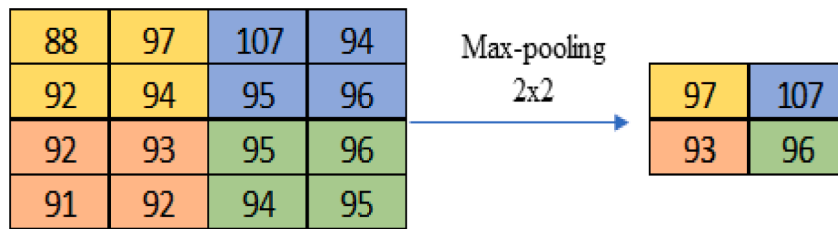


Fig. 9. Max-pooling operation with filter 2x2.

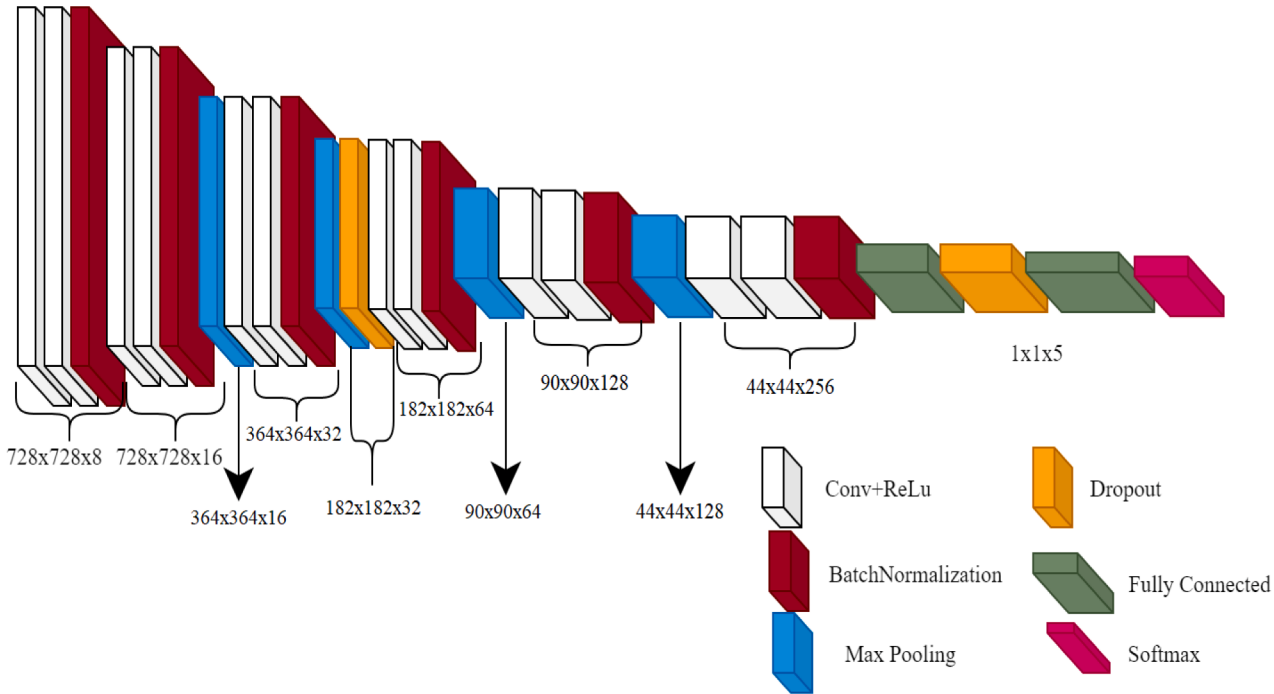


Fig. 10. Proposed Light-SoilNet network architecture.

performing an adaptive histogram is 392.

The pre-processing techniques like HSV histogram, color moment, and Discrete wavelet transform techniques are tested in classifying the soil types. The mentioned techniques perform operations on colour images, and the colour of the soil varies from region to region based on the environment and chemical and climatic conditions. Using texture rather than colour features in classifying the soil types gives the best results. In this paper, we have chosen R, G, and B channels separately rather than as RGB color channels to extract the features. The Adaptive histogram highlights the edges and corner features of the image. The 'V' value has been chosen among HSV color space as it indicates the brightness of the color that varies with the saturation which again gives a grey channel image with color brightness. The performance of the model is better in classifying the soil types using mentioned features.

The HSV color space represents the hue (H), saturation (S), and value (V). HSV histogram is applied to the augmented ROI images by quantizing the hue, saturation, and value with $6 \times 3 \times 5$ equal bins. Among the HSV images, value (V) represents the brightness perception of a specific color. The value images are considered in identifying the texture of the soil samples. RGB channels are extracted from the soil color images to highlight the texture of the soil in each channel (Kumar & Thiagarasu, 2018) The number of soil images generated after HSV and RGB channel extraction is 392 and 1176, respectively.

After pre-processing the soil images, the total number of images generated for training and testing the Light-SoilNet architecture is 1960. Fig. 8 shows the pre-processed sample images of the adaptive histogram,

RGB and V extraction from HSV. Fig. 9.

4.2. Light-SoilNet network architecture

The proposed Light-SoilNet architecture comprises multiple layers for the classification of soil by reducing the number of parameters and increasing the model's efficiency. The layers used in the architecture are the convolution layer, ReLU, batch normalization, max-pooling, dropout, fully connected, and softmax layer. The network is a non-linear model with dominant model characterization capabilities due to its unique convolution, and the pooling structure can extract essential features from sophisticated input information.

4.3. Convolutional layer

The convolutional layer contains filters whose parameters need to be learned to perform the convolutional operations on the input images. 2-D convolutional operation is used for two-dimensional soil images. The smaller size kernel filters are used in the proposed model to extract the spatial features: edges and corners of the soil images. For an input image of size $m \times n$, the output feature map size can be calculated using Eqs. (2) and (3), for which the kernel filter size is $h \times w$.

$$cw_{out} = \frac{(m - ((w - 1) \times d_w + 1) + 2 \times p_w + 1)}{S_w} \quad (2)$$

Table 1

Proposed SoilNet Architecture with parameters and filter values at each layer.

Size/Operation	Activation	Filter	Depth	Stride	No. of Parameters
Input (728×728×1)	–	–	–	–	0
Conv1 + ReLU	728×728×8	2×2	8	1	40
Normalization	728×728×8	–	–	–	16
Conv2 + ReLU	728×728×16	2×2	16	–	528
Normalization	728×728×16	–	–	–	32
Max Pooling	364×364×16	2×2	–	2	0
Conv3 + ReLU	364×364×32	2×2	32	1	2080
Normalization	364×364×32	–	–	–	64
Max Pooling	182×182×32	2×2	–	2	0
Dropout (rate 0.25)	182×182×32	–	–	–	0
Conv4 + ReLU	182×182×64	3×3	64	1	18,496
Normalization	182×182×64	–	–	–	128
Max Pooling	90×90×64	3×3	–	2	0
Conv5 + ReLU	90×90×128	3×3	128	1	73,856
Normalization	90×90×128	–	–	–	256
Max Pooling	44×44×128	3×3	–	2	0
Conv6 + ReLU	44×44×256	2×2	256	1	131,328
Normalization	44×44×256	–	–	–	512
FC7	1×5	–	–	–	2,478,085
Dropout (rate 0.3)	1×5	–	–	–	0
FC8	1×5	–	–	–	30
Softmax	1×5	–	–	–	0

Table 2

System specifications.

Hardware\Software	Specifications
Memory (RAM)	16 GB
Processor	Intel Core i7-8700 CPU @3.20 GHz
Graphics	NVIDIA GeForce GT710
Operating system	Windows 10 Pro, 64 bit

Table 3

Dataset Description for training and testing.

Class Label	Training images	Testing images
Clay	344	146
Loam	250	100
Sandy Loam	250	100
Loamy Sand	294	126
Sand	244	106

$$ch_{out} = \frac{(n - ((h - 1) \times d_h + 1) + 2 \times p_h)}{S_h} + 1 \quad (3)$$

Where, cw_{out} and ch_{out} are the width and height of the convolution layer output, respectively.

p_w and p_h are the padding size in the horizontal and vertical ends of the input dimensions.

d_w and d_h are the dilation factors.

4.3.1. Batch Normalization

To speed up the training of the SoilNet model, batch normalization is used after the convolutional layer. It improves the performance and stability of the training model, reduces the covariate shift and achieves efficient learning in the model.

4.3.2. Pooling

In the Light-SoilNet network, the max-pooling layer of size 2×2 and 3×3 with stride two is used to reduce the network depth and learnable parameters. Max-pooling layer with convolution layers helps in position invariant feature detection.

4.3.3. Dropouts

Neural networks trained on relatively small datasets can overfit the training data. Dropouts are utilized to minimize overfitting and achieve regularization in the Light-SoilNet network. Dropouts are added to drop a fraction of neurons of the model randomly, which makes the model not rely on one input as it might be dropped out at random. Neurons will not learn redundant details of input. This makes the next layer neuron that takes input from these neurons not create a bias as it does not depend on dropout neurons completely. The next layer of neurons has inputs from other existing neurons. In the proposed model, we have used the dropouts with a lower rate at the hidden layers to minimize co-adaptions required for learning and provide better results by avoiding overfitting for the imbalanced data.

The classification of soils is done based on the probability values of the softmax layer. The proposed network is set to classify five different types of soils: sand, clay, loam, sandy loam and loamy sand.

The proposed Light-SoilNet architecture comprises six convolutional, ReLU and batch normalization layers, four max-pooling layers, two dropout and fully connected layers and one softmax in classifying the soil types. The Light-SoilNet architecture is shown in Fig. 10. Table 1 depicts the learnable parameters and activations of the layers used in developing the lightweight architecture.

The dimensions of the layers filters and functions are chosen after simulating with different dimensions for best accuracy values. As the number of images of the five soil classes is not equal, the soil classes with fewer images are assigned a higher weight factor, and the classes with more images are given a lower weight factor. The whole network is trained using backpropagation using an automatic differentiation technique by utilizing the Adam mini-batch gradient descent optimizer to update the model parameters. To maximize accuracy, the network depth is typically increased in research studies. On the other hand, as network depth grows, so does the frequency with which gradient vanishing and gradient exploding occur (Rehmer & Kroll, 2020). This will directly affect network accuracy. Classification accuracy can be improved by striking a balance between network size, number of layers, and image resolution (Tan & Le, 2019). The image resolution of 728×728 has provided better results than 512×512 .

The soil dataset created is less in the number of images for each class, and classifying using deep networks would lead to performance degradation. To avoid these conditions, a lightweight network is designed. Dropout layers are included in the middle and final layers by varying the dropout range from 0.2 to 0.3 to avoid vanishing gradients. The experiments give better soil classification results with a mini-batch size of 32 and a learning rate of 0.01. The validation accuracy is enhanced and reduced the over-fitting of the data encountered initially by using dropout layers of factors 0.25 and 0.3 at layers 13 and 26, respectively.

5. Results & analysis

This section discusses the training and testing implementation of the proposed model and evaluates the obtained results with different performance parameters. The performance The Light-SoilNet architecture is implemented using Deep Learning (DL) toolbox, which assists in visualizing the network activations and monitoring the network training progress. Table 2 depicts the system specifications used to implement the proposed model. The performance analysis and comparative analysis of the proposed network are discussed by comparing them with the lightweight pre-trained and conventional pre-trained DL networks. In the proposed model, the Light-SoilNet network was adopted to classify five types of soil. The architecture is designed by conducting repetitive experiments to increase the performance of the model and reduce the number of parameters. The lack of publicly available datasets makes comparison with other datasets unachieved.

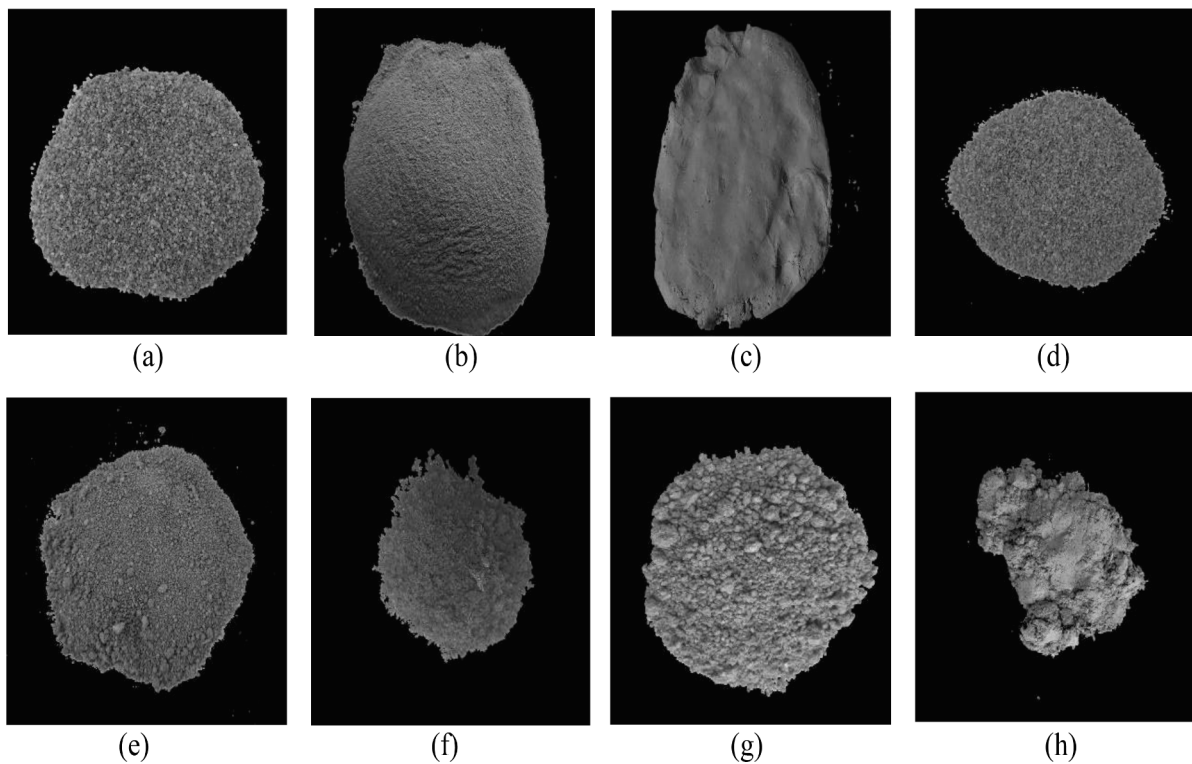


Fig. 11. Sample training images of soil. (a,b) Sand (c,d) Clay (e,f) Loamy sand (g) Sandy loam (h) Loam.

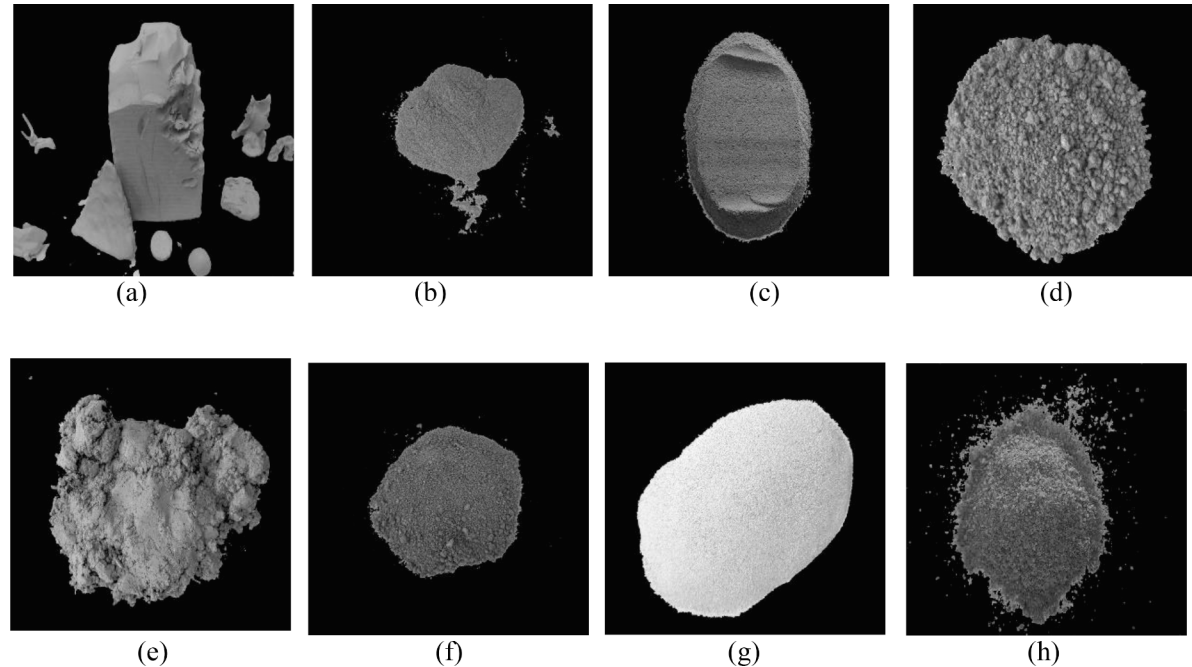


Fig. 12. Sample testing images of soil. (a-c) Clay (d) Sandy loam (e) Loam (f) Loamy sand (g,h) Sand.

5.1. Training and testing

To train the SoilNet network, the dataset with 1960 images for five different soil classes is created. The dataset developed by augmenting and pre-processing the IRSID database is divided into 70:30 for training and testing purposes. Among the dataset, 1382 images are used for training, and 578 are used for testing validation. [Table 3](#) depicts the images of each class split for training and testing of the network.

The proposed SoilNet architecture is trained with 70 % of the available dataset. [Fig. 11](#) shows the sample soil images used for training. During the training of the model, the learning rate of the model is set to 0.01 with a validation frequency of 30. A total of 8 epochs with 12 iterations per epoch are used to train the model. During the training, the texture features of the soil images are extracted automatically by the convolutional and pooling layers. The weights of the network are updated for each iteration during the training phase. The extracted

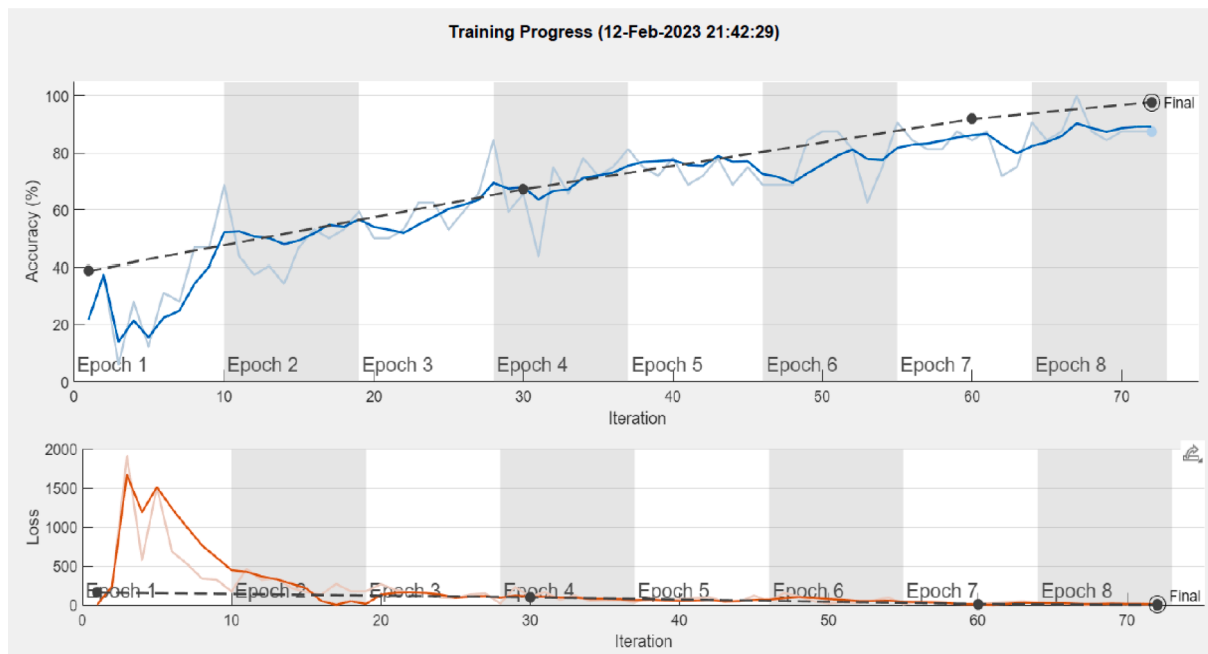


Fig. 13. Training progress of the Light-SoilNet architecture.

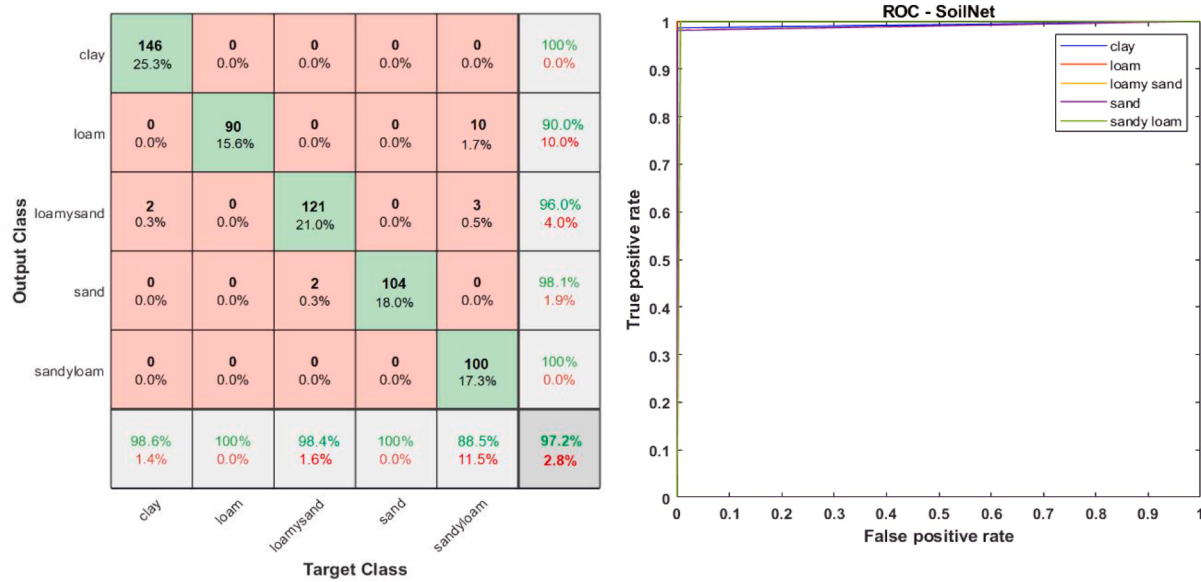


Fig. 14. Confusion matrix and ROC of the Light-SoilNet network.

Table 4
Performance metrics of the proposed model for each class.

Class	TP	TN	FP	FN	Precision	Recall	F1 score
Clay	146	430	0	2	1.000	0.986	0.993
Loam	90	478	10	0	0.900	1.000	0.947
Sandy Loam	100	465	0	13	1.000	0.885	0.939
Loamy Sand	121	454	5	2	0.960	0.984	0.972
Sand	104	476	0	2	1.000	0.981	0.990

features are used in classifying the appropriate soil class using fully connected and softmax layers.

For testing the proposed network, 334 images of the five soil classes were used. Fig. 12 shows the sample testing images of the soil. The proposed SoilNet network classifies the five soil classes effectively. The

overall accuracy of the proposed SoilNet network is 97.20 % in classifying five different types of soil images. The Light-SoilNet network takes 11 s in testing the 334 soil images of size $728 \times 728 \times 1$. Fig. 13 shows the training progress of the proposed model.

5.2. Performance indicators

The performance metrics calculated in evaluating the model are precision, recall, F1-score and accuracy. The parameters used to assess the performance metrics are True positive (T_p), True negative (T_N), False positive (F_p) and False negative (F_N) of the confusion matrix in multi-class classification. Let us consider ' i ' to be each actual class, ' j ' to be the predicted class, X be the confusion matrix and n is the number of classes. The parameters can be calculated as:

Table 5

Ablation experiment results for preprocessed techniques.

Adaptive Histogram	V value	RGB Channels	Accuracy	F1 Score				
				Clay	Loam	Loamysand	Sand	Sandyloam
-	✓	✓	81.4	0.83	0.92	0.95	0.64	0.82
✓	-	✓	78.4	0.79	0.50	0.92	0.86	0.55
✓	✓	-	92.8	0.94	0.75	0.88	0.95	1.00
✓	✓	✓	97.2	0.99	0.94	0.97	0.99	0.94

Table 6

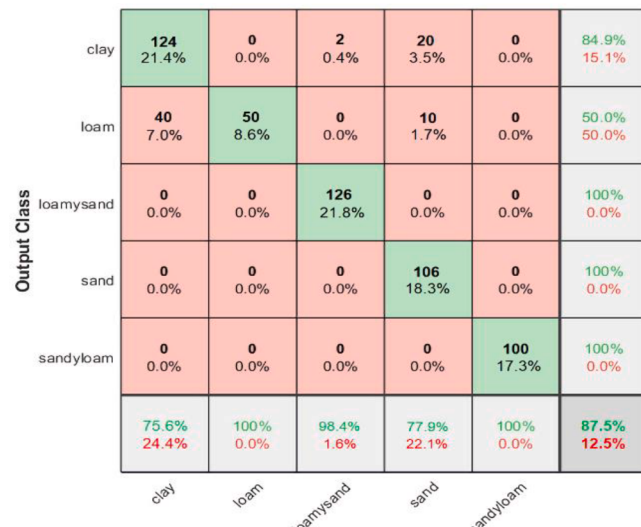
Classification accuracy of Light-SoilNet and pre-trained lightweight networks.

Architecture	Accuracy (%)	Size (MB)
Proposed model	97.20	9.62
MobileNet-v2	95.45	21.5
MobileNet-v3	94.5	21.1
EfficientNet-B0	87.54	28.3
ShuffleNet	95.67	14.5

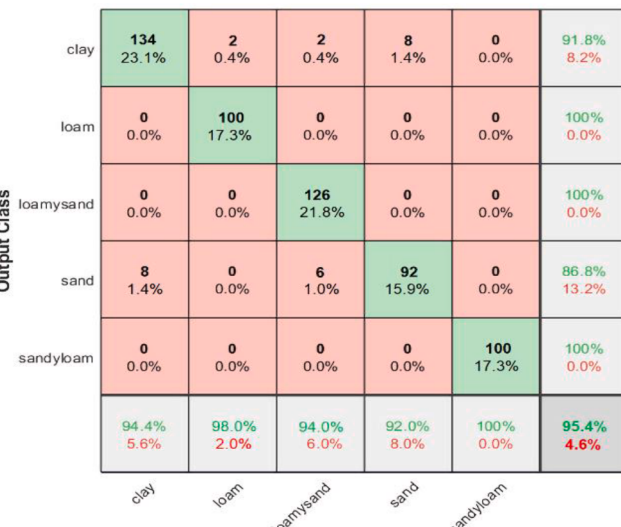
$$T_P(i) = X_{i,i} \quad (4)$$

$$F_N(i) = \sum_{j=1}^n X_{i,j} - T_P(i) \quad (5)$$

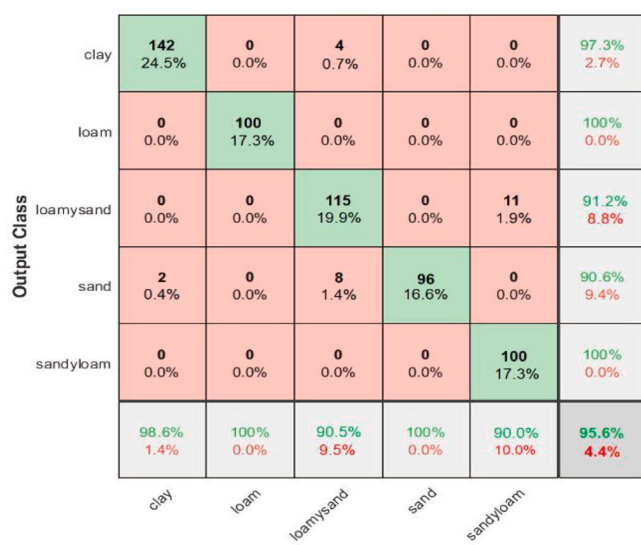
$$F_P(i) = \sum_{j=1}^n X_{j,i} - T_P(i) \quad (6)$$



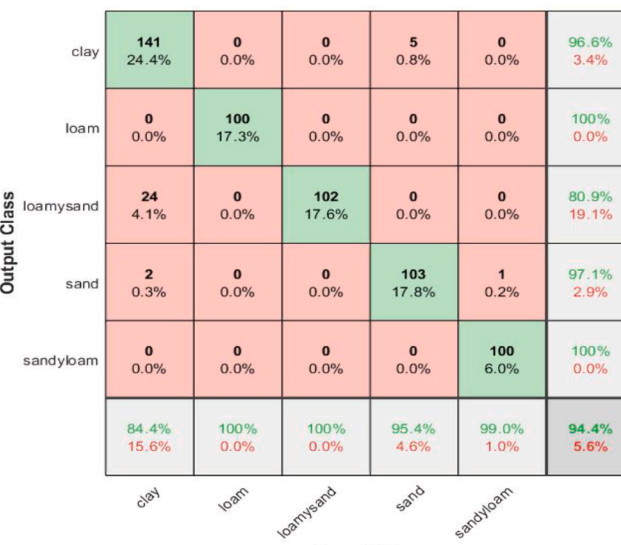
(a)



(b)



(c)



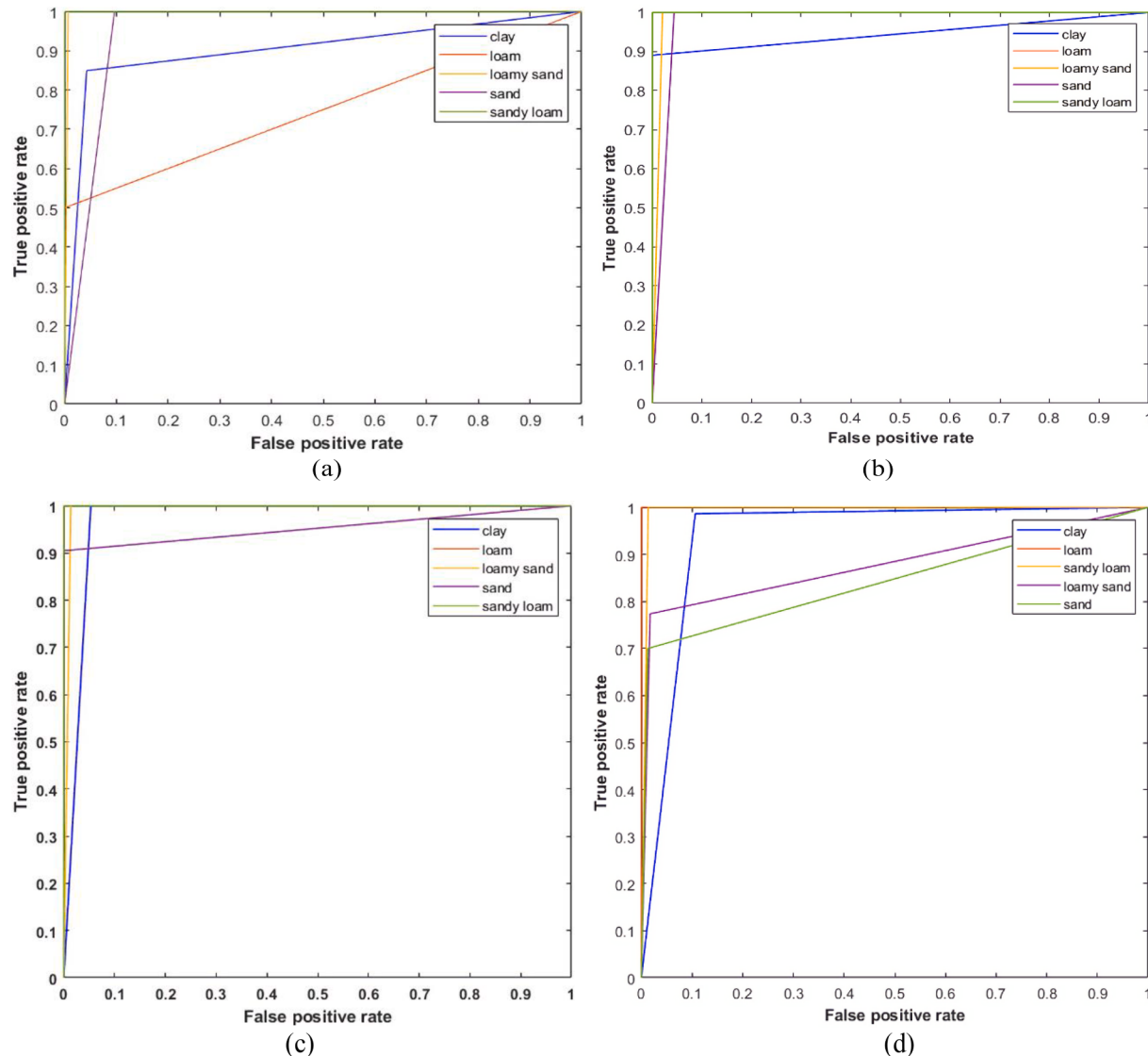
(d)

Fig. 15. Confusion matrix. (a) EfficientNet-B0 (b) MobileNet-v2 (c) ShuffleNet (d) MobileNet-v3.

Table 7

Performance analysis for the five soil classes with pre-trained lightweight networks.

Network	Clay		Loam		Sand		Sandy loam		Loamy sand	
	Precision	Recall	Precision	Recall	Precision	Recall	Precision	Recall	Precision	Recall
MobileNet-v2	0.918	0.944	1	0.980	0.885	0.920	1	1	1	0.940
ShuffleNet	0.973	0.986	1	1	0.906	1.000	1	0.901	0.913	0.906
EfficientNet-B0	0.849	0.756	0.500	1	1	0.779	1	1	1	0.984
Light-SoilNet	1	0.986	0.900	1	1	0.981	1	0.885	0.960	0.984

**Fig. 16.** ROC of (a) EfficientNet-B0 (b) MobileNet-v2 (c) ShuffleNet (d) Proposed Light-SoilNet.**Table 8**

Classification accuracy with comparative results.

Architecture	Accuracy (%)	Parameters (Millions)	FLOPs (G)	Inference Time (sec)	Training Time (min)	Size (MB)
Proposed model	97.20	2.7	3.74	11	16	9.62
Inception-v3	94.46	24	5.72	6.5	6.5	94.1
Vgg-19	85.12	144	15.47	7	7.1	519
ResNet-50	94.46	23	3.87	4.5	6	100
AlexNet	91.00	61	7.27	4.1	7.4	226

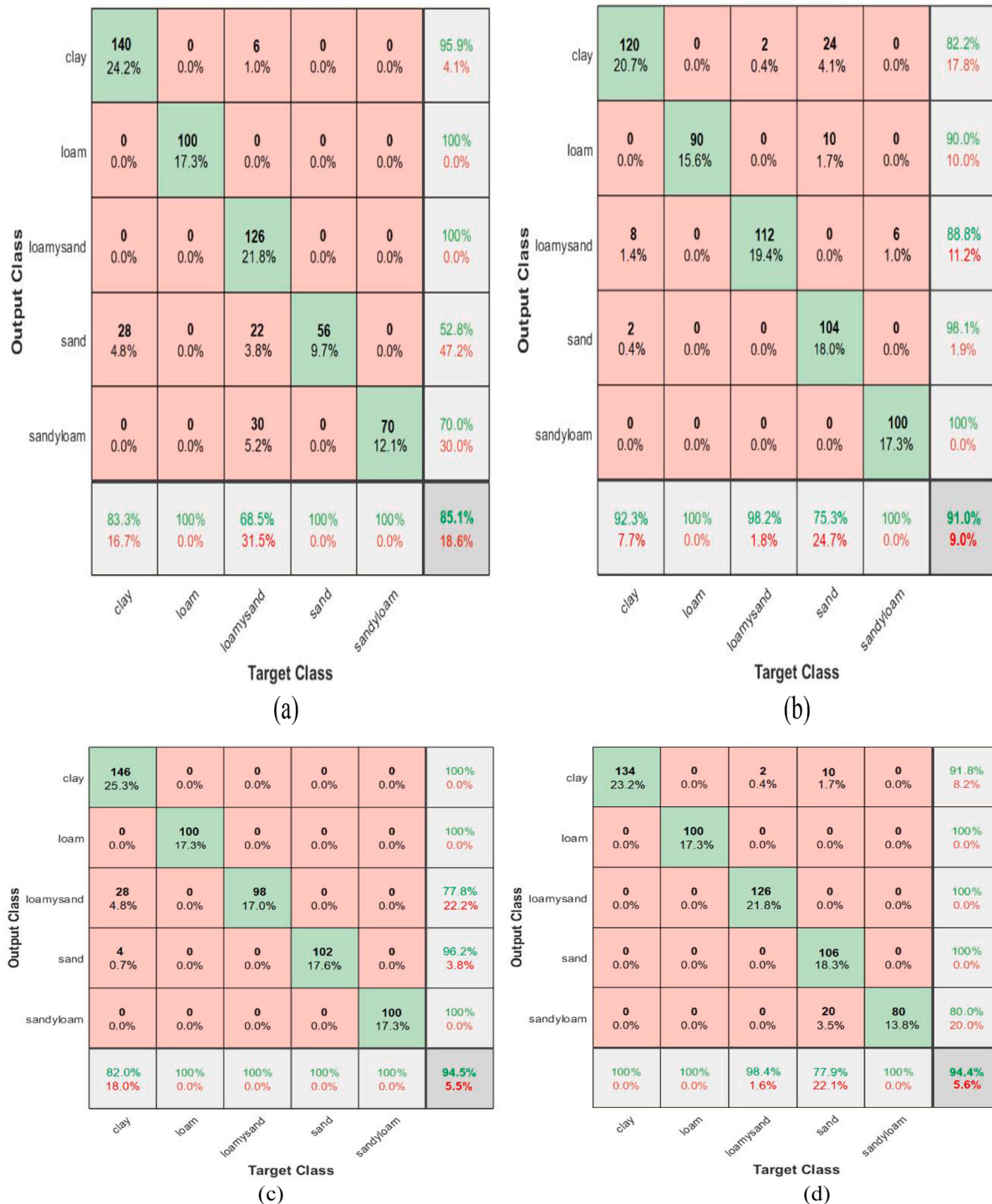


Fig. 17. Confusion matrix. (a) VGG-19. (b) AlexNet. (c) ResNet-50. (d) Inception-v3.

$$T_N(i) = \sum_{j=1}^n \sum_{i=1}^n X_{ij} - T_P(i) - F_p(i) - F_N(i) \quad (7)$$

Precision indicates the positive predicted values, which is the ratio of T_p and all positive values. It is calculated and measured by using the equation

$$Precision_i(P) = \frac{T_p(i)}{T_p(i) + F_p(i)} \quad (8)$$

The role of recall is how efficiently the model can predict the relevant data. Recall tells the true positive rate of the model, also called the

sensitivity of the model.

$$Recall_i(R) = \frac{T_p(i)}{T_p(i) + F_N(i)} \quad (9)$$

When there is an unequal class distribution and the need to balance between precision and recall, then a better F1-score indicates good precision and recall. F1-score indicates the harmonic mean of precision and recall.

$$F1Score = \frac{2 \times Precision_i \times Recall_i}{Precision_i + Recall_i} = \frac{2 \times T_p(i)}{2 \times T_p(i) + F_p(i) + F_N(i)}$$

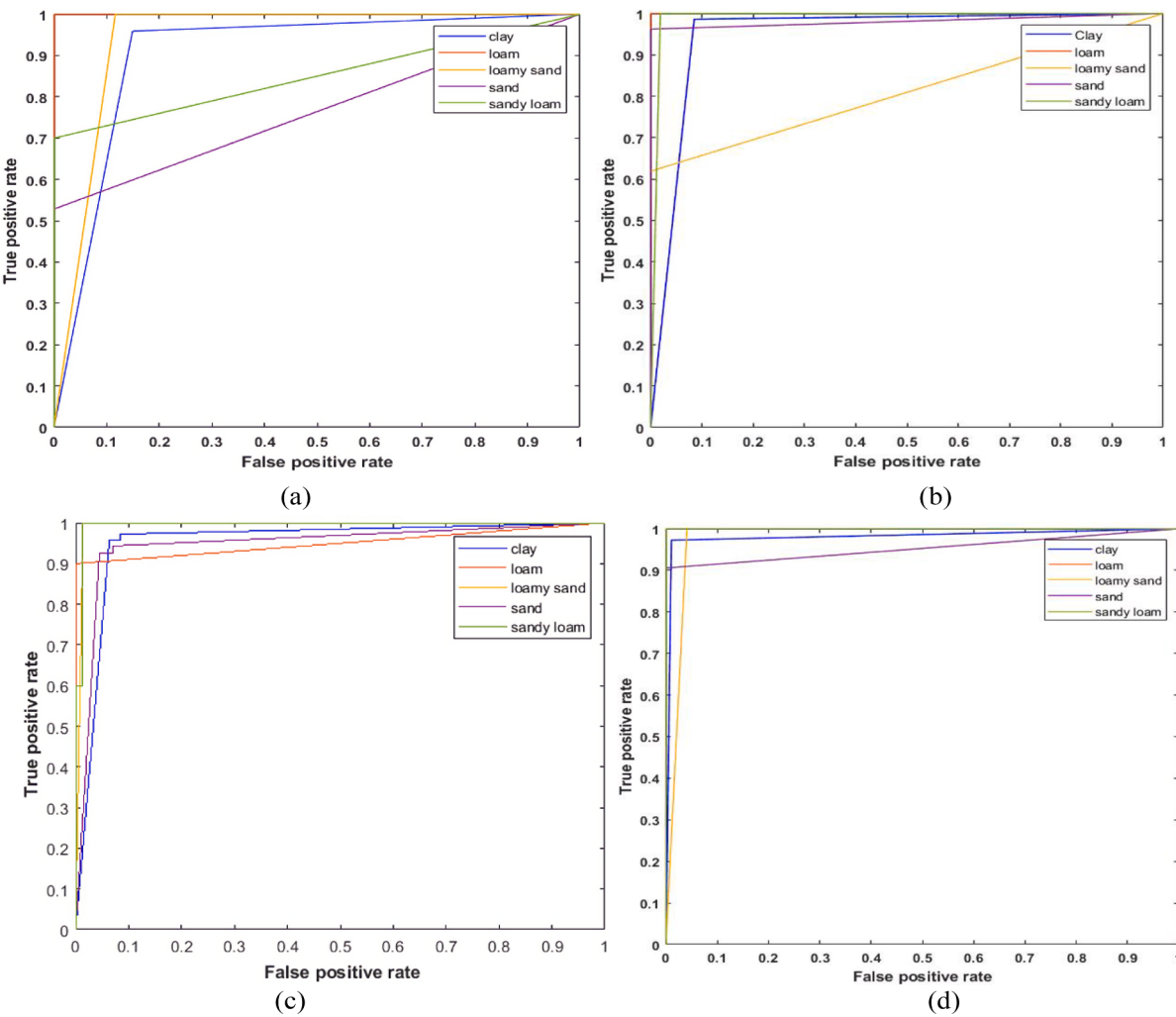


Fig. 18. ROC of (a) VGG-19. (b) AlexNet (c)ResNet-50 (d) Inception-v3.

Table 9
Performance analysis for the five soil classes with pre-trained DL networks.

Network	Clay		Loam		Sand		Sandy loam		Loamy sand	
	Precision	Recall	Precision	Recall	Precision	Recall	Precision	Recall	Precision	Recall
AlexNet	0.822	0.923	0.900	1	0.981	0.754	1.000	1	0.889	0.982
Inception	0.918	1	1	1	1	0.779	0.800	1	1	0.984
Vgg-19	0.959	0.833	1	1	0.528	0.651	0.700	1	1	0.685
ResNet-50	1	0.820	1	1	0.962	1	1	1	0.778	1.000
Light-SoilNet	1	0.986	0.900	1	1	0.981	1	0.885	0.960	0.984

$$\text{Accuracy} = \frac{T_P(i)}{T_P(i) + F_P(i) + F_N(i) + T_N(i)} \quad (11)$$

The performance parameters and metrics are calculated by using the confusion matrix generated while testing the Light-SoilNet network. Fig. 14 shows the confusion matrix and ROC of the proposed model multiclass soil classification. The confusion matrix calculates the metrics like the true positive, true negative, false positive, false negative, precision, recall, and F1-score of the network. The performance parameters and metrics of the proposed model are depicted in Table 4.

5.3. Ablation experiment

Ablation experiments are conducted on the proposed Light-SoilNet model for the preprocessed soil images, and the results are shown in

Table 5. The soil classification without preprocessed adaptive histogram images is 81.4 %, without V-value is 78.4 %, and without RGB channels images is 92.8 % using the proposed model. Using the three pre-processed images increased the proposed model accuracy to 97.20 %, and the F1 scores of each soil type are improved.

5.4. Performance analysis with lightweight networks

The lightweight SoilNet network performance is compared with existing pre-trained lightweight networks like MobileNet-v2, ShuffleNet, and EfficientNet-B0 (Michele et al., 2019; Synced, 2017; Chowdhury et al., 2021). The performance of the Light-SoilNet network is comparably higher than these pre-trained lightweight networks. Table 6 shows the accuracy of the pre-trained lightweight networks compared with the proposed network. Fig. 15 shows the confusion

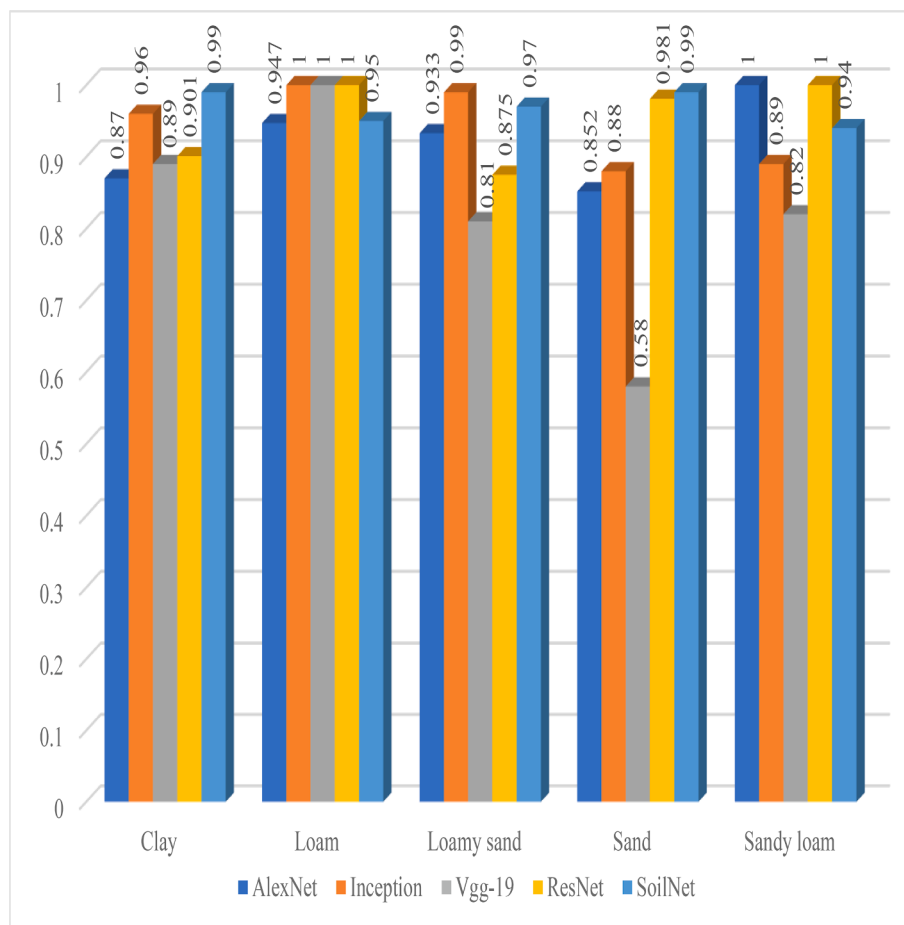


Fig. 19. Comparative analysis of F1-score for the soil images.

matrix generated for the pre-trained lightweight networks. The performance metrics are calculated using the confusion matrix for the existing lightweight DL networks. The performance metrics of the pre-trained lightweight networks and the proposed model are tabulated in Table 7. Fig. 16 shows the ROC generated for the proposed Light-SoilNet network and the pre-trained lightweight DL networks. It shows that Light-SoilNet achieves impressive results compared to other pre-trained lightweight networks. The soil dataset is tested with the advanced pre-trained lightweight network ShuffleNet-V2 and the performance in classifying the soil type is 97.8 % which is 0.6 % higher than the proposed Light-SoilNet model.

5.5. Performance analysis with pre-trained DL networks

The Light-SoilNet network and the state-of-the-art models such as Inception-v3, Vgg-19, ResNet-50, and AlexNet are compared to prove the efficiency of the proposed network (Victor Ikechukwu et al., 2021; Islam et al., 2018; Xiao et al., 2020; Krizhevsky et al., 2012). Table 8 shows that the Light-SoilNet architecture can generalize significantly better than conventional pre-trained DL networks. Specifically, due to its ability to extract multi-scale features, the Light-SoilNet model achieves a 2.7 % higher classification performance than the state-of-the-art network trained exclusively on the same soil dataset. The number of parameters of the Light-SoilNet network is comparatively very low than the other DL networks. The inference time to test the soil dataset, training time, and network size are mentioned in Table 8. The Light-SoilNet network achieves higher classification results when compared to state-of-the-art networks. Validation is performed using several evaluation metrics, including accuracy, precision, recall, and F1 score

indicators. The confusion matrix generated for the pre-trained DL models in classifying the soil types is shown in Fig. 17. Fig. 18 shows the ROC generated for the pre-trained DL networks.

The performance metrics like precision and recall of the pre-trained DL networks for each soil class are calculated using confusion matrixes. Table 9 summarizes the performance metrics, like the precision and recall of each soil class for the proposed model and the state-of-the-art DL networks. From Table 9, the performance metric F1-score has been calculated to evaluate the performance of the model. The F1-score of each soil class of each model is compared, and the same is shown in Fig. 19.

The comparative results of the F1-score show that the proposed model performed better in classifying the clay and sand soils than the pre-trained networks. The F1-score in classifying soil types loam, loamy, and sandy loam is achieved high in the pre-trained DL networks than in the proposed network. The number of soil images available for loam, loamy sand, and sandy loam is less, leading to a decrease in the F1 score compared with existing pre-trained DL networks.

The proposed model performance was evaluated at each epoch by comparing it with pre-trained DL and lightweight networks. Fig. 20 shows the accuracy graph achieved by the models at each epoch. Fig. 20 shows that the proposed model has competed with the pre-trained DL and lightweight networks in terms of accuracy at each epoch. Consistently the proposed model performance has increased in achieving high performance than the state-of-the-art.

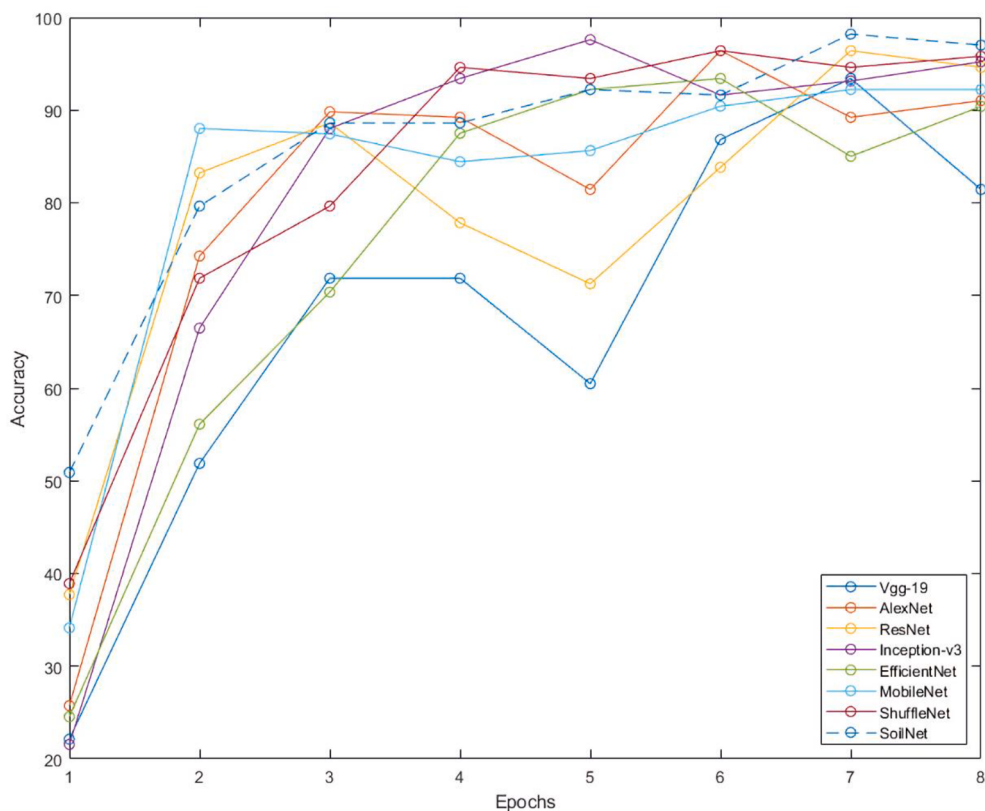


Fig. 20. Comparison of Light-SoilNet with the pre-trained DL and lightweight networks using accuracy as cross-validation.

5.6. Comparison of state-of-the-art

5.6.1. With neural network models

Table 10 shows the state-of-the-art artificial neural networks (ANN), CNN and DL networks in classifying the soil types. (Mengistu & Alemayehu, 2018) along with the digital camera images, moisture sensor data was used in soil classification. ANN with backpropagation was used to classify and produced less accuracy. The author (Inazumi et al., 2020b) used CNN in classifying the digital camera soil images of three soil types and achieved 82 % accuracy, which is less than the other DL methods. (Azizi et al., 2020) used stereo pair images in classifying the soil aggregates of size varying from 7 mm to 110 mm diameter with ResNet-50, Vgg-16 and Inception-v4 and reported 98.72 %, 97.12 % and 95.83 % accuracy, respectively. The proposed Light-SoilNet model has given an accuracy of 97.20 % in classifying the soils of size varying from 0.425 mm to 0.002 mm in diameter.

The IRSID soil dataset was created by following the standards and online soil image dataset where the images were randomly collected from various sources have been tested with the (Inazumi et al., 2020b; Azizi, 2020), and proposed Light SoilNet models in classifying the soil types. The online soil images were captured by not following standards in capturing the images and the images were blurry. Table 11 shows the performance of IRSID and the online dataset with the proposed and existing models. The IRSID dataset has given better performance with the existing models than the online dataset. For soil image classification, certain standards need to be followed to achieve better performance.

5.6.2. With machine learning models

Table 10 shows the state-of-the-art machine-learning models for classifying soil types using various soil images. The authors (Srunitha & Padmavathi, 2017; Barman & Choudhury, 2020) used mobile camera images to classify the soil types. The texture features extracted from the soil images were classified with Support Vector Machine (SVM) and Multi SVM classifier algorithms and achieved 74.4 % and 91.37,

respectively, comparably less than the proposed model. (Chung et al., 2012) used CCD camera images, which helped in identifying the RGB characteristics of the soil to classify the soil types using the Linear regression (LR) algorithm, and achieved 96 % of accuracy less than ours. Smartphone-based classification sensor to classify the soil colour used by (P. Han et al., 2016). Based on the wavelength of the colour, the soil classification was done using Linear discriminant analysis (LDA) and achieved 97.2 % accuracy, similar to the Light-SoilNet model, but the colours of the soil vary with the chemical properties of the soil is a drawback in classification. (Vibhute et al., 2016) classified the soil types based on colour by using hyperspectral images. The classification was done using the Radial Basis function SVM which yields less accuracy.

CNNs have been used in various architectures outperforming conventional ML models such as ANNs or LR, LDA and SVMs. However, difficulties in comparing the efficacy of the different CNN architectures arise because each of the techniques, as mentioned earlier, uses a dataset that is not publicly available due to privacy reasons. We present a straightforward comparison between the proposed SoilNet model and almost all well-known DL architectures and lightweight networks using the same dataset created for the soil classification problem to overcome this barrier. The overall accuracy of the proposed Light-SoilNet network is 97.20 % which is 1.2 % higher compared with pre-trained DL and lightweight networks.

Even though the proposed Light-SoilNet model uses a relatively less soil image dataset, this work suggests soil classification using mobile images, incorporating various pre-processing techniques to highlight the features of the soil images. The outcomes of the proposed Light-SoilNet model indicate the feasibility of classifying agricultural soils by using mobile images.

The following summarises the significant outcomes of this research article: In all aspects like computational performance, complexity, and generalization, the proposed Light-SoilNet architecture outperforms the state-of-the-art models in image classification of the soil. Most significantly accomplished DL models are generally trained and verified on

Table 10

Comparison of the result with state-of-the-art of machine learning and neural network models.

Model	Image type	Soil types	No of soils	Accuracy
ResNet-50	Stereo pair images	Soil aggregate (micro and macro aggregate soils)	6	98.72
Vgg-16				97.12
Inception				95.83
CNN	Digital camera	Sand, clay, gravel	3	82
ANN	CPT data	Fine-grained soils (sandy clay, clay, clayey sand)	3	89.47
ANN	Digital camera & moisture sensor data	--	6	89.7
SVM	Smartphone images	Silty Sand, Clay Sand, Sand Clay, Clay, Humus Clay, Clay Peat, Peat	7	74.4
MultiSVM	Smartphone images	Sand, Clay, Loam, Silt loam, Loamy sand, sandy loam, clay loam, sandy clay loam, silt clay, silt clay loam, Loam fine sand, silt loam	12	91.37
Linear Regression	CCD Camera images	Clay, Loam, silt clay loam, clay loam, silt loam	5	96
Radial Basis function SVM	Hyperspectral images	Brown Sandy soil, Black sandy soil, Black Clay soil, Red sandy soil, Gray clay soil	2	71.18
Linear Discriminant Analysis	Android mobile camera with spectrometer lens	Red soil, yellow soil, Drab soil, Podzolic soil, Desert soil, Chernozem, Paddy soil, Purple soil	9	97.2
PLS-DA SVM	LASER-Induced Breakdown Spectroscopy (LIBS) Data	Rock soil	6	88.3
Proposed (Light-SoilNet)	Smartphone images	Clay, sand, loam, loamy sand, sandy loam	7	91.67
Proposed (Light-SoilNet)	Smartphone images	Clay, sand, loam, loamy sand, sandy loam	5	97.20

Table 11

Comparison of the Light-SoilNet and IRSID dataset with existing models and online dataset.

Model	IRSID Dataset Accuracy (%)	Online Dataset Accuracy (%)
(Azizi, 2020)ResNet-50	94.46	68.1
(Azizi, 2020)Vgg-16	92.8	57.4
(Azizi, 2020)Inception-v3	94.46	68.09
(Inazumi, Ph, 2020)	92.72	70.2
Proposed (Light-SoilNet)	97.2	65.7

extremely large quantities of data. The proposed Light-SoilNet model is validated on a small dataset that could be considered a limitation of this work. As the network is portrayed as a black box, the inability of the current method in explaining decisions might be seen as a shortcoming. In terms of performance metrics, the SoilNet model performance is high in the classification of sand and clay. When it comes to loam, sandy loam, and loamy sand, the performance metrics of the proposed model are less with some of the existing DL and lightweight networks. After analysing the metrics and the model, the reason for less accuracy for the three soil types is:

- The number of soil images collected for loam, sandy loam, and loamy sand soil types is less.
- The texture of the soil types loam, sandy loam, and loamy sand of the collected samples appear the same.

The proposed model has performed a little lower in classifying the loam, loamy sand and sandy loam soil types when compared with the pre-trained DL networks Vgg-19, AlexNet, ResNet-50, and Inception-v3.

6. Conclusion & future work

This paper presents a new lightweight CNN-based network architecture for classifying the five different types of soil images. Soil image database IRSID was created, where soil images are captured by acquiring soil samples from various regions of Andhra Pradesh, India. The collected soil samples are tested in the soil mechanics laboratory using sieve analysis and hydrometer methods to determine the texture of the soil. The proposed Light-SoilNet network was used to classify five different types of soils. The performance of the model compared with pre-trained lightweight and DL pre-trained networks The accuracy of the proposed model is effectively high compared with the state-of-the-art. The true positive rate of loam and loamy sand is low due to fewer soil images of these classes. The Light-SoilNet model performance was measured with various performance metrics like accuracy, precision, recall, and F1-score for each soil category which shows that the proposed model performs better compared to each class with lightweight networks and pre-trained DL models. Better performance was achieved by reducing the parameters and complexity of the system. The computational time of the proposed Light-SoilNet network is higher than the pre-trained DL and lightweight networks. The weights of the pre-trained DL and lightweight networks are pre-defined, whereas, for the proposed network, the weights have to be updated during the model training and testing, which leads to more computational time.

In future research, the classification accuracy of soil types loam, sandy loam and loamy sand by the proposed Light-SoilNet network will be improved compared with the DL networks. The number of soil images to classify the soil type will be increased by collecting more soil samples from organized soil and agriculture fields. The proposed model will be extended to evaluate the on-site soil samples by ensuring the time and cost of processing the samples.

Declaration of Competing Interest

The authors declare that they have no known competing financial interests or personal relationships that could have appeared to influence the work reported in this paper.

Data availability

Data will be made available on request.

References

- Alary, K., Babre, D., Cancer, L., Feder, F., Szwarc, M., Naudan, M., & Bourgeon, G. (2013). Pretreatment of soil samples rich in short-range-order minerals before particle-size analysis by the pipette method. *Pedosphere*, 23(1), 20–28. [https://doi.org/10.1016/S1002-0160\(12\)60076-9](https://doi.org/10.1016/S1002-0160(12)60076-9)
- Krizhevsky, A., Sutskever, I., & Hinton, G. E. (2012). ImageNet Classification with Deep Convolutional Neural Networks. *Advances in Neural Information Processing Systems*, 25, 1097–1105.
- Azizi, A., Gilandeh, Y. A., Mesri-Gundoshmian, T., Saleh-Bigdeli, A. A., & Moghaddam, H. A. (2020a). Classification of soil aggregates: A novel approach based on deep learning. *Soil and Tillage Research*, 199(January). <https://doi.org/10.1016/j.still.2020.104586>
- Azizi, A., Gilandeh, Y. A., Mesri-Gundoshmian, T., Saleh-Bigdeli, A. A., & Moghaddam, H. A. (2020b). Classification of soil aggregates: A novel approach based on deep learning. *Soil and Tillage Research*, 199(March 2019). <https://doi.org/10.1016/j.still.2020.104586>.

- Barman, U., & Choudhury, R. D. (2020). Soil texture classification using multi class support vector machine. *Information Processing in Agriculture*, 7(2), 318–332. <https://doi.org/10.1016/j.inpa.2019.08.001>
- Benjamin E. Backus. (2018). *Soil Hydrometer Testing, Easy Guide for Hydrometer Analysis - Gilson Co.* <https://www.globalgilson.com/blog/soil-hydrometer-analysis>.
- Cervantes-Godoy, D., Dewbre, J., Amegnaglo, C. J., Soglo, Y. Y., Akpa, A. F., Bickel, M., Sanyang, S., Ly, S., Kuiseu, J., Ama, S., Gautier, B. P., Odudo-ofori, E., Aboagye Anokye, P., Acquaye, N. E. A., Danelar, V. M., Mineo, J., Fadipe A.E.A., *Amolegbe K.B. and Afun O.O., Ganiev, I., Maguire, C., ... Meena, M. S. (2014). The future of food and agriculture: trends and challenges. In *The future of food and agriculture: trends and challenges* (Vol. 4, Issue 4).
- K. Chatterjee M.S. Obaidat D. Samanta B. Sadoun S.K.H. Islam R. Chatterjee Classification of Soil Images using Convolution Neural Networks 2021 and Informatics (CCCI), 1–5.
- Chen, Z., Chen, J., Ding, G., & Huang, H. (2023). A lightweight CNN-based algorithm and implementation on embedded system for real-time face recognition. *Multimedia Systems*, 29(1), 129–138.
- Cheng, J., Wu, J., Leng, C., Wang, Y., & Hu, Q. (2017). Quantized CNN: A unified approach to accelerate and compress convolutional networks. *IEEE Transactions on Neural Networks and Learning Systems*, 29(10), 4730–4743.
- Chowdhury, N. K., Kabir, M. A., Rahman, M. M., & Rezoana, N. (2021). ECOVNet: A highly effective ensemble based deep learning model for detecting COVID-19. *Peer Computer Science*, 7, 1–25. <https://doi.org/10.7717/PEERJ-CS.551>
- Chung, S. O., Cho, K. H., Cho, J. W., Jung, K. Y., & Yamakawa, T. (2012). Soil texture classification algorithm using RGB characteristics of soil images. *Journal of the Faculty of Agriculture, Kyushu University*, 57(2), 393–397. <https://doi.org/10.3182/20101206-3-jp-3009.00005>
- D N Kiran, P., Murugan, R., & Tripti, G. (2021). Indian Regions Soil Image Database (IRSID): A dataset for classification of Indian soil types | IEEE DataPort. *IEEE Dataport, DOI: <https://dx.doi.org/10.21227/2zz3-F173>*.
- David C. L. Gatiboni, J. M. (2018). *Soils and Plant Nutrients*. Chapter 1. In: K.A. Moore, and L.K. Bradley (Eds). North Carolina Extension Gardener Handbook; Raleigh, NC. <https://content.ces.ncsu.edu/extension-gardener-handbook/1-soils-and-plant-nutrients>.
- Denil, M., Shakibi, B., Dinh, L., Ranzato, M., & de Freitas, N. (2013). Predicting parameters in deep learning. *Advances in Neural Information Processing Systems*, 26.
- Dorothee Spuhler; Nina Carle. (2019). Crop Selection | SSWM - Find tools for sustainable sanitation and water management! <https://sswm.info/sswm-solutions-bop-markets/improving-water-and-sanitation-services-provided-public-institutions-0/crop-selection>.
- Fomin, D., Timofeeva, M., Ovchinnikova, O., Valdes-Korovkin, I., Holub, A., & Yudina, A. (2021). Energy-based indicators of soil structure by automatic dry sieving. *Soil and Tillage Research*, 214(August), Article 105183. <https://doi.org/10.1016/j.still.2021.105183>
- Gómez-Ríos, A., Tabik, S., Luengo, J., Shihavuddin, A. S. M., Krawczyk, B., & Herrera, F. (2019). Towards highly accurate coral texture images classification using deep convolutional neural networks and data augmentation. *Expert Systems with Applications*, 118, 315–328. <https://doi.org/10.1016/j.eswa.2018.10.010>
- Gong Y., Liu L., Yang M., & Bourdev L. (2014). Compressing deep convolutional networks using vector quantization. *ArXiv Preprint ArXiv:1412.6115*.
- Haider W., ur Rehman A., Nouman Durrani M., Karachi F., & Sadiq ur Rehman P. (2019). Knowledge based Soil Classification Towards Relevant Crop Production. *IJACSA International Journal of Advanced Computer Science and Applications*, 10(12).
- Han, P., Dong, D., Zhao, X., Jiao, L., & Lang, Y. (2016). A smartphone-based soil color sensor: For soil type classification. *Computers and Electronics in Agriculture*, 123, 232–241. <https://doi.org/10.1016/j.compag.2016.02.024>
- Han S., Mao H., & Dally W.J. (2015). Deep compression: Compressing deep neural networks with pruning, trained quantization and huffman coding. *ArXiv Preprint ArXiv:1510.00149*.
- He, K., Zhang, X., Ren, S., & Sun, J. (2015). Spatial pyramid pooling in deep convolutional networks for visual recognition. *IEEE Transactions on Pattern Analysis and Machine Intelligence*, 37(9), 1904–1916.
- Howard, A. G., Zhu, M., Chen, B., Kalenichenko, D., Wang, W., Weyand, T., Andreetto, M., & Adam, H. (2017). Mobilenets: Efficient convolutional neural networks for mobile vision applications. *ArXiv Preprint ArXiv:1704.04861*.
- Inazumi, S., Intui, S., Jotisankasa, A., Chaiprakaikew, S., & Kojima, K. (2020a). Artificial intelligence system for supporting soil classification. *Results, Engineering*, 8 (November). <https://doi.org/10.1016/j.rineng.2020.100188>
- Inazumi, S., Ph, D., Intui, S., Eng, M., Jotisankasa, A., Ph, D., Chaiprakaikew, S., Ph, D., & Kojima, K. (2020b). Artificial intelligence system for supporting soil classification. *Results, Engineering*, 8(October). <https://doi.org/10.1016/j.rineng.2020.100188>
- Islam, M. S., Foysal, F. A., Neelam, N., Karim, E., & Hossain, S. A. (2018). IncepPTB: A CNN based classification approach for recognizing traditional Bengali games. *Procedia Computer Science*, 143, 595–602. <https://doi.org/10.1016/j.procs.2018.10.436>
- Jagetia, A., Goenka, U., Kumari, P., & Samuel, M. (2022). Visual Transformer for Soil Classification. *IEEE Students Conference on Engineering and Systems (SCES), 2022*, 1–6.
- Jayanthi, P., & Iyyanki, M. (2019). Extraction of Tumor Chunk Using Image Segmentation: Thresholding and HSV Color Space. *International Conference on Advances in Computational Intelligence and Informatics*, 119, 1–7. https://doi.org/10.1007/978-981-15-3338-9_1
- Kumar E.B., & Thiagarasu V. (2018). Color channel extraction in RGB images for segmentation. *Proceedings of the 2nd International Conference on Communication and Electronics Systems, ICCES 2017*, 2018-Janua(Icces), 234–239. <https://doi.org/10.1109/CESYS.2017.8321272>.
- Lanjewar, M. G., & Gurav, O. L. (2022). Convolutional Neural Networks based classifications of soil images. *Multimedia Tools and Applications*, 81(7), 10313–10336.
- Liu, S., Zhang, M., Feng, F., & Tian, Z. (2020). Toward a "Green Revolution" for Soybean. *Molecular Plant*, 13(5), 688–697. <https://doi.org/10.1016/j.molp.2020.03.002>
- Lu, N., Ristow, G. H., & Likos, W. J. (2000). The Accuracy of Hydrometer Analysis for Fine-Grained Clay Particles. *Geotechnical Testing Journal*, 23(4), 487–495. <https://doi.org/10.1520/gtj11069j>
- Mengistu, A. D., & Alemanyehu, D. M. (2018). Soil characterization and classification: A hybrid approach of computer vision and sensor network. *International Journal of Electrical and Computer Engineering*, 8(2), 989–995. <https://doi.org/10.11591/ijece.v8i2.pp989-995>
- Michele, A., Colin, V., & Santika, D. D. (2019). Mobilenet convolutional neural networks and support vector machines for palmprint recognition. *Procedia Computer Science*, 157, 110–117. <https://doi.org/10.1016/j.procs.2019.08.147>
- Reale, C., Gavín, K., Librić, L., & Jurić-Kaćunić, D. (2018). Automatic classification of fine-grained soils using CPT measurements and Artificial Neural Networks. *Advanced Engineering Informatics*, 36(September 2017), 207–215. <https://doi.org/10.1016/j.aei.2018.04.003>
- Rehmer, A., & Kroll, A. (2020). On the vanishing and exploding gradient problem in Gated Recurrent Units. *IFAC-PapersOnLine*, 53(2), 1243–1248.
- Sashi Gulhati; Ranjan, G. T. S. N. (1986). Methods of test for soils: Part 4 grain size analysis. In *Indian Standards: Vol. IS: 2720*. Bureau of Indian Standards.
- Singh, K., Vishwakarma, D. K., Walia, G. S., & Kapoor, R. (2016). Contrast enhancement via texture region based histogram equalization. *Journal of Modern Optics*, 63(15), 1444–1450. <https://doi.org/10.1080/09500340.2016.1154194>
- Soil Types: A Main Aspect Of Agricultural Productivity.* (2019). <https://eos.com/blog/soil-types-as-a-paramount-aspect-of-agricultural-productivity/>.
- Srunitha K., & Padmavathi S. (2017). Performance of SVM classifier for image based soil classification. *International Conference on Signal Processing, Communication, Power and Embedded System, SCOPES 2016 - Proceedings*, 411–415. <https://doi.org/10.1109/SCOPES.2016.7955863>.
- Sudhakar, S. (2017). *Histogram Equalization | by Shreenidhi Sudhakar | Towards Data Science*. <https://towardsdatascience.com/histogram-equalization-5d1013626e44>.
- Synced. (2017). *ShuffleNet: An Extremely Efficient Convolutional Neural Network for Mobile Devices*. Medium. <https://medium.com/syncedreview/shufflenet-an-extremely-efficient-convolutional-neural-network-for-mobile-devices-72c6f5b01651>.
- Tan, M., & Le, Q. (2019). Efficientnet: Rethinking model scaling for convolutional neural networks. *International Conference on Machine Learning*, 6105–6114.
- Uddin, M., & Hassan, M. R. (2022). A novel feature based algorithm for soil type classification. *Complex & Intelligent Systems*, 8(4), 3377–3393.
- USDA. (2013). *Soil Texture Calculator | NRCS Soils*. https://www.nrcs.usda.gov/wps/portal/nrcs/detail/soils/survey/?cid=nrcs142p2_054167.
- Vibhute, A. D., Kale, K. V., Dhumal, R. K., & Mehrotra, S. C. (2016). Soil type classification and mapping using hyperspectral remote sensing data. *Proceedings - 2015 International Conference on Man and Machine Interfacing, MAMI 2015*, 1, 1–4. <https://doi.org/10.1109/MAMI.2015.7456607>.
- Victor Ikechukwu, A., S. M., R. D., & RC, S. (2021). ResNet-50 vs VGG-19 vs Training from Scratch: A comparative analysis of the segmentation and classification of Pneumonia from chest x-ray images. *Global Transitions Proceedings*. <https://doi.org/10.1016/j.gltip.2021.08.027>.
- von der Goltz, J., Dar, A., Fishman, R., Mueller, N. D., Barnwal, P., & McCord, G. C. (2020). Health Impacts of the Green Revolution: Evidence from 600,000 births across the Developing World. *Journal of Health Economics*, 74, Article 102373. <https://doi.org/10.1016/j.jhealeco.2020.102373>
- Wu, J., Leng, C., Wang, Y., Hu, Q., & Cheng, J. (2016). Quantized convolutional neural networks for mobile devices. *Proceedings of the IEEE Conference on Computer Vision and Pattern Recognition*, 4820–4828.
- Xiao, J., Wang, J., Cao, S., & Li, B. (2020). Application of a Novel and Improved VGG-19 Network in the Detection of Workers Wearing Masks. *Journal of Physics: Conference Series*, 1518(1). <https://doi.org/10.1088/1742-6596/1518/1/012041>
- Yang, J., Zhang, L., Tang, X., & Han, M. (2022). CodNet: A lightweight CNN architecture for detection of COVID-19 infection. *Applied Soft Computing*, 130, Article 109656.
- Yu, Y., Xu, T., Shen, Z., Zhang, Y., & Wang, X. (2019). Compressive spectral imaging system for soil classification with three-dimensional convolutional neural network. *Optics Express*, 27(16), 23029. <https://doi.org/10.1364/oe.27.023029>
- Zhang, T., Wang, Z., Li, F., Zhong, H., Hu, X., Zhang, W., Zhang, D., & Liu, X. (2023). Automatic detection of surface defects based on deep random chains. *Expert Systems with Applications*, 229. <https://doi.org/10.1016/j.eswa.2023.120472>
- Zhang, W. J., Yang, G., Lin, Y., Ji, C., & Gupta, M. M. (2018). On definition of deep learning. *World Automation Congress (WAC), 2018*, 1–5.
- Zhao, L., Wang, L., Jia, Y., & Cui, Y. (2022). A lightweight deep neural network with higher accuracy. *PLoS One*, 17(8), e0271225.